Ph.D. dissertation examination presentation

이미지를 이용한 기계학습 기반
해상 상태 예측
Sea state prediction based on machine learning using images

Yun-Ho Kim
14 June 2022

Computational Mechanics and Structural Systems
Department of Mechanical Engineering
Korea Advanced Institute of Science and Technology

Advisor: Prof. Phill-Seung Lee

KAIST

Contents

BACKGROUNDS

- Maritime accidents

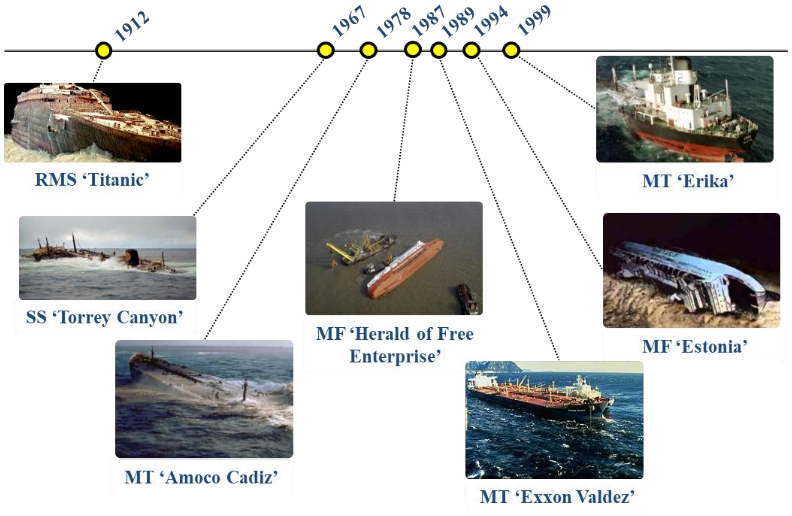

[Major maritime accidents related to the enactment and revision of SOLAS]

- MF: Motor Fishing ship
- MT: Motor Tanker
- RMS: Royal Mail Steamer
- SS: Steam Ship

[Oryong-501 sinking (2014)]

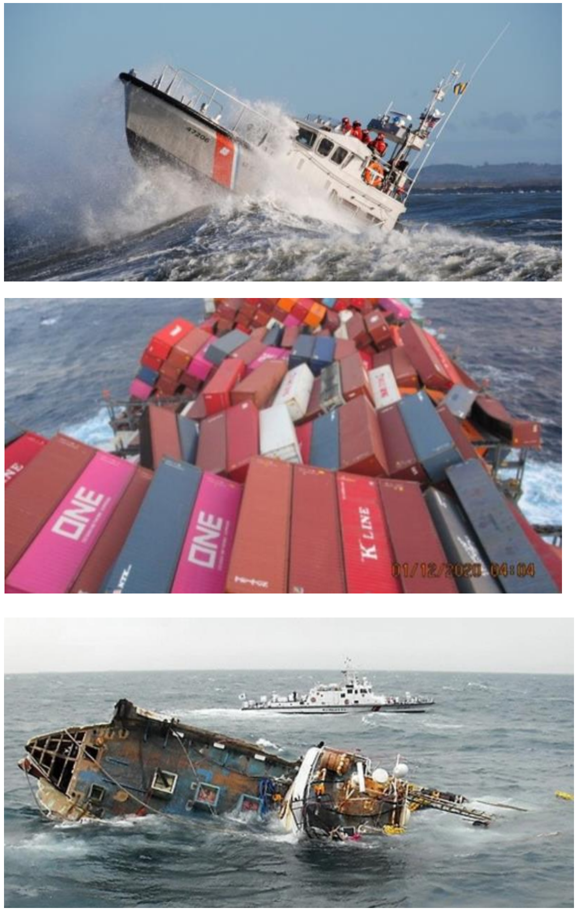

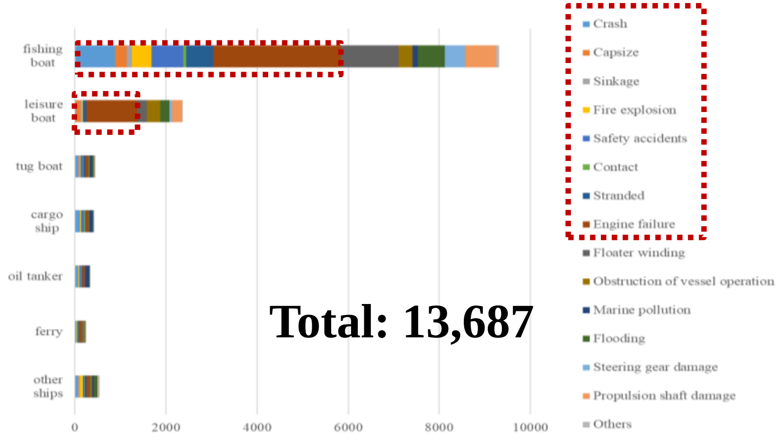

Total: 13,687

Source: The impact of major maritime accidents on the development of international regulations concerning safety of navigation and protection of the environment(2017), Daniel Duda and Ryszard Wawruch, Scientific Journal of Polish Naval Academy, 4(211), 23-44.
Oryong 501 sinking incident in the Bering Sea-International DVI cooperation in the Aisa Pacific(2017), Nak-Eun Chung et al., Forensic Science International, 278, 367-373.
Ministry of Oceans and Fisheries/ Central Maritime Safety Tribunal Maritime/ Accident Statistical Yearbook
https://www.kmst.go.kr/kmst/statistics/annualReport/selectAnnualReportList.do#a

CONVENTIONAL OCEAN ENV. MEASUREMENTS

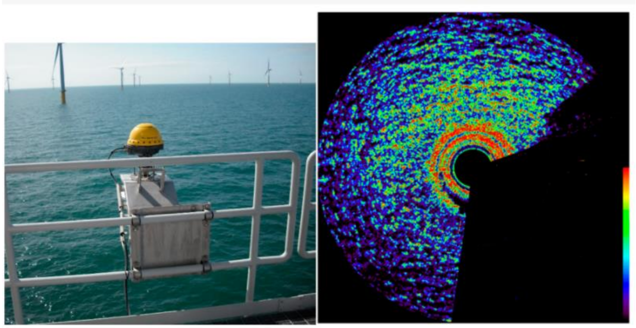

[Radar-based system]

Setup cost: 50,000~200,000 USD

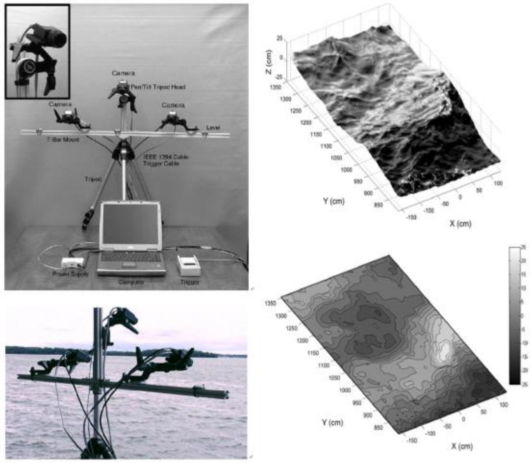

[Image-based system]

Setup cost: 10,000~50,000 USD

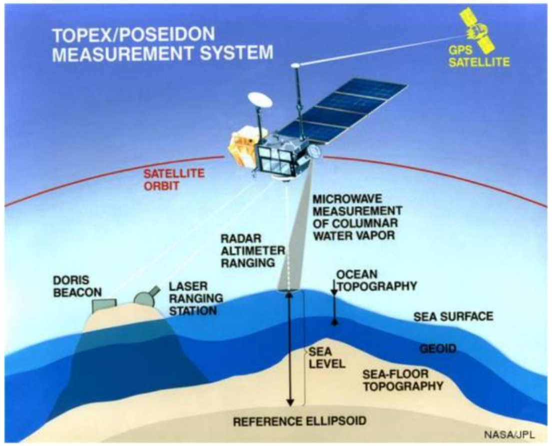

[Satellite wave measurement]

Utilization cost: less than 10,000 USD per operation

Resolution: over 500m

Item (using X-band radar)		**Unit**	**Country**	**Insititute**	**Technical characteristics**		
					Range	**Resolution**	**STD**
Wave	height	Hs [m]	Norway, Denmark	MIROS OceanWaves	**0.5 ~ 20**	0.1	10%
	period	Tp [s]	Norway, Denmark	MIROS OceanWaves	**3.0 ~ 20**	0.1	5%
	direction	[deg]	Norway, Denmark	MIROS OceanWaves	**0 ~360**	1	10%
Wind	direction	[deg]	Denmark	GKSS	**Corr. = 0.99**		14.24°
	speed	[m/s]	Denmark	GKSS	**Corr. = 0.97**		0.85m/s
Current	direction	[deg]	Norway	MIROS	**1 ~ 360**	1	7%
	speed	[m/s]	Norway	MIROS	**0.0 ~ 2.5**	0.01	0.05m/s
Bilateral flow		number	US, Japan	Oregon univ. Tsukuba univ.	in developing		

Source: MIROS website (https://www.miros-group.com/)
Satellite wave measurements for coastal engineering applications(1999), Harald EK and Stephen FB, Coastal Engineering, 37(3-4), 283-307.
Piepmeier et al., 2006. 2006-2364: A stereo vision-based wave surface measurement project. 2006 Annual Conference & Exposition, Chicago, USA.

SEA STATE CLASSIFICATION

Source: Principle of Naval Architecture Vol.III
DNV-RP-C205. Environmental conditions and environmental loads
Douglas sea scale(1921) → WMO sea state

- **Sea state classification by significant wave height**

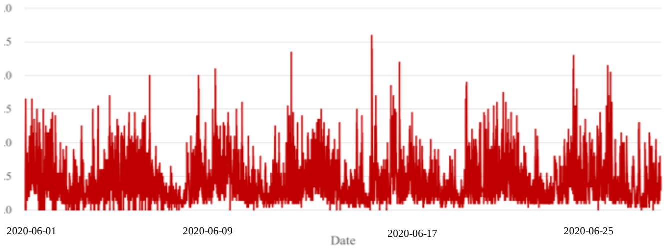

[Time series of wave]

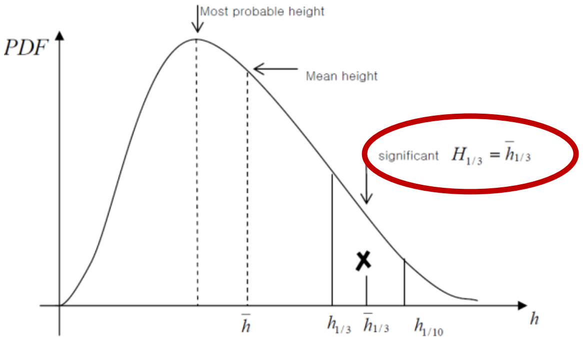

[PDF of wave amplitude]

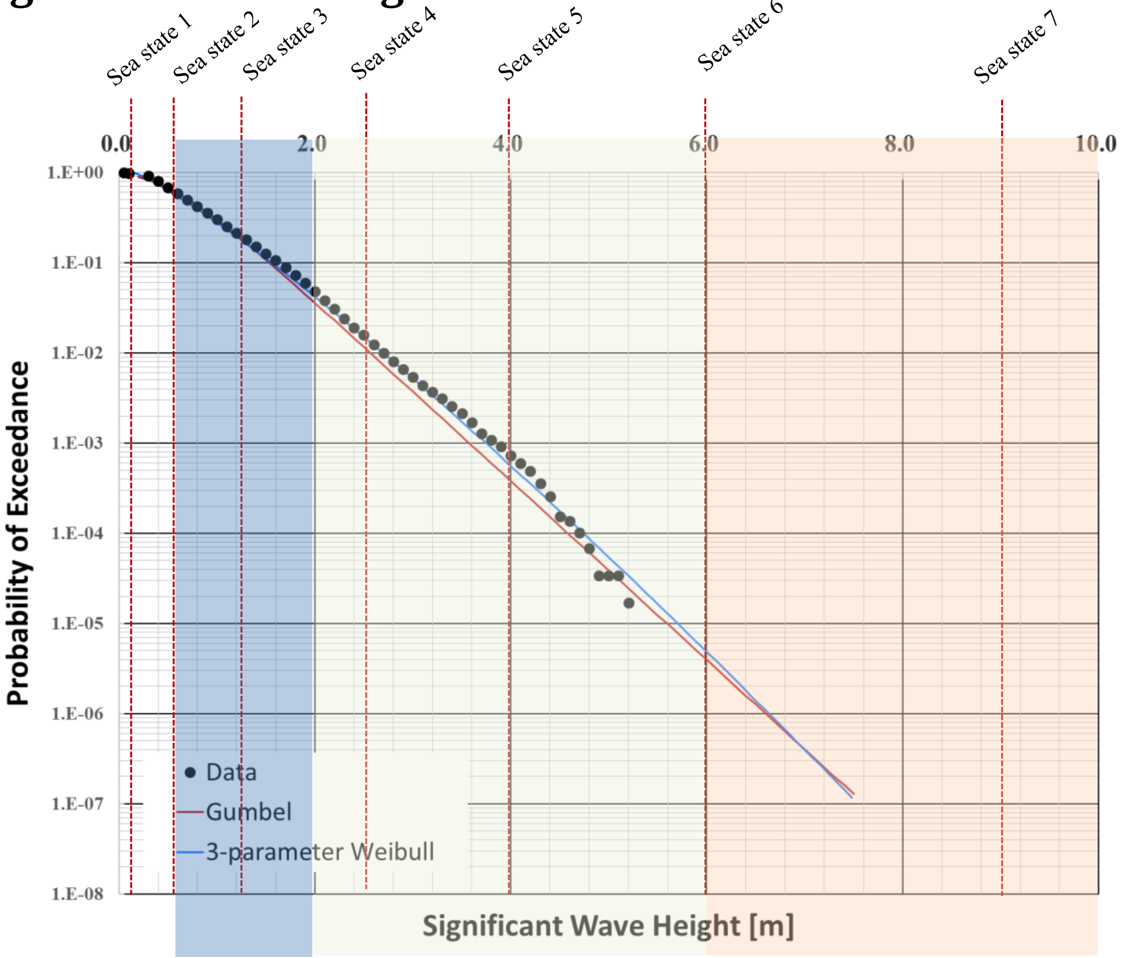

Roll resonance region for small ships(<50m)

Roll resonance region for middle-sized ships(<150m)

Roll resonance region for middle-sized ships(>200m)

- Initially heuristic classification
- Significant wave height(Hs) is positioned as main physical quantity specifying the sea condition

PROBLEM DEFINITION

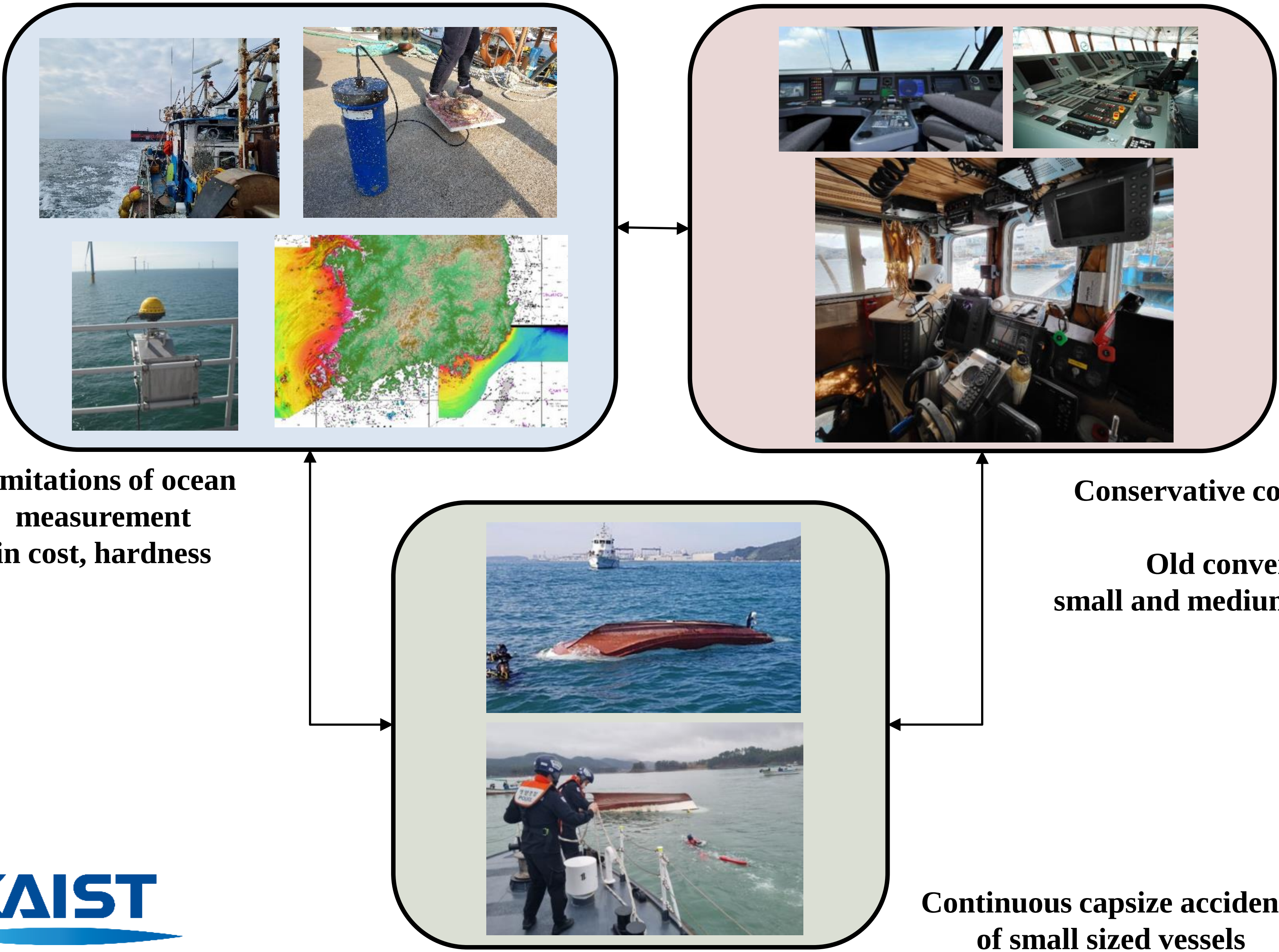

Limitations of ocean measurement
in cost, hardness

Conservative control system

Old conventional
small and medium sized vessels

Continuous capsize accidents
of small sized vessels

PURPOSE OF RESEARCH

Condition1: Significant development in computing H/W → Big data

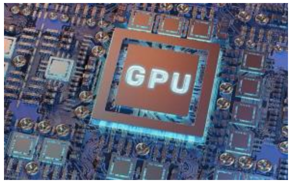

데이터 상세

한국가스공사_동해안 너울성 파도 발생 주기 DATA

동해안 너울성 파도관련 해상 데이터는 기상청 날씨누리 바다예보에서 각각의
고와 파주기를 통해 너울성 파도 발생을 파악
월별, 주별 발생 빈도를 분석하고 이를 토대로 너울성 파도 발생에 대비하여

공공데이터활용지원센터는 공공데이터포털에 개방되는 3단계 이상의 오픈
오픈 API를 활용하기 위해서는 공공데이터포털 회원 가입 및 활용신청이
파일데이터는 로그인 없이 다운로드를 통해 이용하실 수 있습니다.

한국가스공사_동해안 너울성 파도 발생 주기 DATA

파일데이터 정보

파일데이터명	한국가스공사_동해안 너울성 파도 발생 주기 DATA_

Condition2: Overcoming previous short-comings in ML

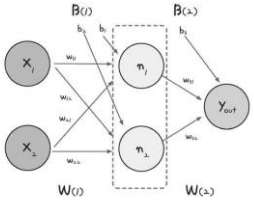

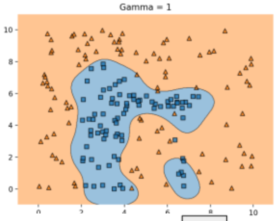

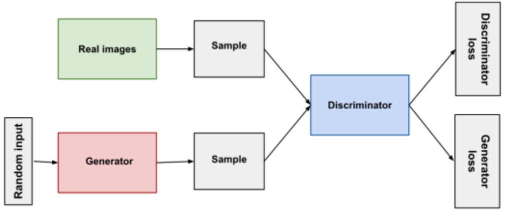

- **Developing the practical ocean environment estimation system with data science**
  1. Constructing the suitable **artificial network**
  2. Estimation of sea states through **real ocean snapshot images**
  3. Evaluating the **applicability and coverage of the network**’s estimation performance

STATE OF THE ART

- **Applications of artificial intelligence in marine engineering**
  - Review articles: Deo(2010), Kutz(2017), Sclavounos and Ma(2018), Ahmad(2019)
  - Performance predictions and fault detections on ships and offshore structures
    - Ramirez et al.(2020), Gheliotis et al.(2020), Berghout et al.(2021), etc.
  - Predictions on wave characteristics
    - Zamani et al.(2008), Mahjoobi et al.(2009), Wei(2017), James et al.(2018), Sarkar et al.(2018), Stringari et al.(2019), etc.
- **Wave classification using machine learning**
  - Liu et al.(2019): Wave height and period classification for 2D waves
  - Buscombe and Carini(2019): Classifying wave breaking phenomena in infrared imagery
  - Masoumi(2021): Ocean data classification in US using unsupervised machine learning for planning hybrid wave-wind offshore energy devices
  - Kim et al.(2021): Transformation to nearshore wave from global wave data using ANN and Group Method of Data Handling(GMDH)
  - Demetriou et al.(2021): Coastal zone significant wave height prediction by ANN and decision tree model
  - **Ravuri et al.(2021): Nowcasting using generative models of radar**

DEEP LEARNING NETWORKS

- **Convolutional Neural Network(CNN)**
  - A network widely used in **image classification** by convolution layers and pooling layers
  - **Convolution layer**: Extract the characteristics contrast structure indicated by the filter from the image
  - **Pooling layer**: After convolution, the maximum in the target square domain represent the dominant characteristics

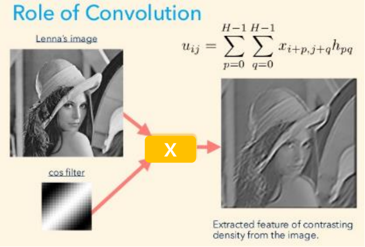

Input image

Convolution Kernel

$$\begin{bmatrix} -1 & -1 & -1 \\ -1 & 8 & -1 \\ -1 & -1 & -1 \end{bmatrix}$$

Feature map

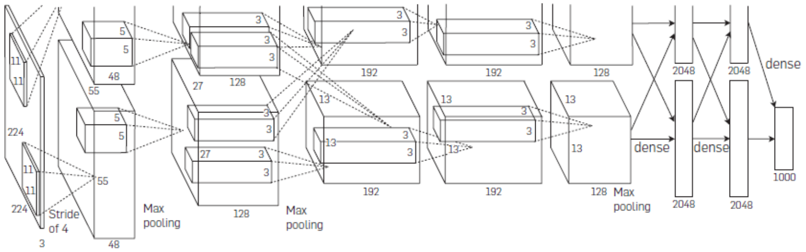

- **Long Short-Term Memory(LSTM)**
  - A special kind of RNN, capable of learning long-term dependencies
  - Remembering information for long periods of time is practically their default behavior, not something they struggle to learn.
  - **Forget, input, output gates & cell state per 1 hidden layer**

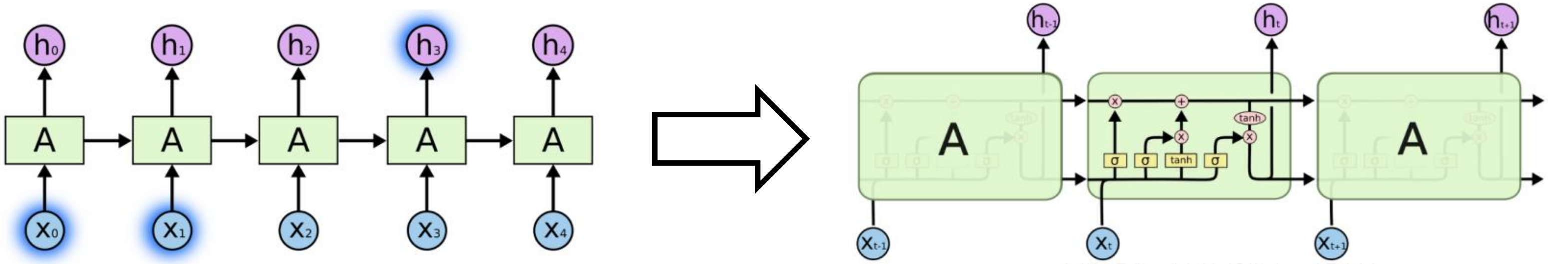

Source:
Alex, K., Ilya, S., and Geoffrey, E.H., 2017, "ImageNet classification with deep convolutional neutral networks," Communications of the ACM, 60(6), 84-90.
Hochreiter, S., Schmidhuber, J., 1997. Long Short-Term Memory. Neural Computation. 9(8), 1735-1780. http://www.bioinf.jku.at/publications/older/2604.pdf.

CNN STRUCTURE(PRELIMINARY)

Per each RGB channel

	Original	CONV_01	Pool_01	CONV_02	Pool_02	CONV_03	Pool_03	CONV_04
Height(I)	656	654	164	162	41	39	10	8
Width(I)	875	873	219	217	55	53	14	12
Depth	1	16	16	512	512	32,768	32,768	2,097,152
Number of weight		144		41,472		23,887,872		13,759,414,272
Number of biases		16		512		32,768		2,097,152

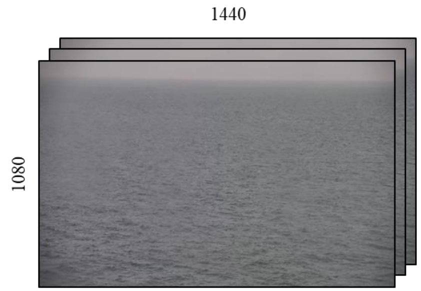

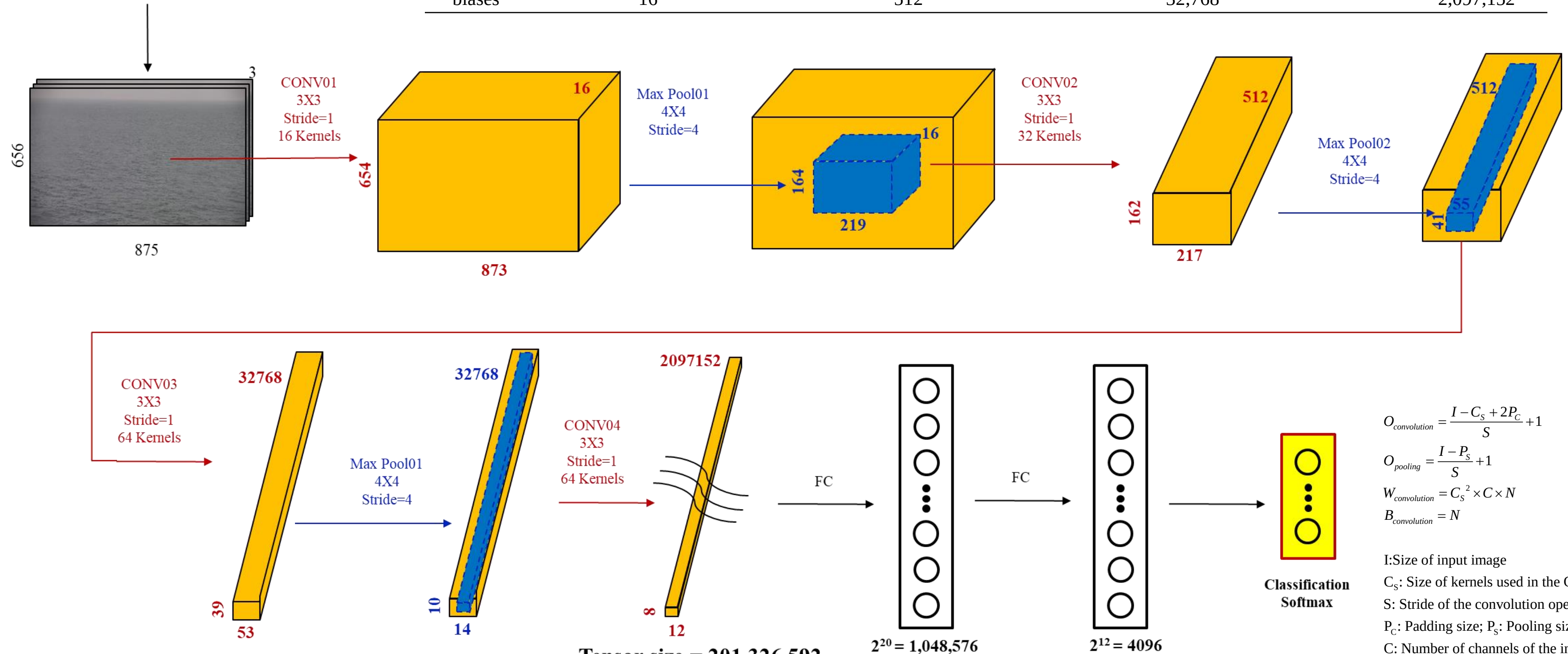

Tensor size = 201,326,592

$$O_{convolution} = \frac{I - C_S + 2P_C}{S} + 1$$

$$O_{pooling} = \frac{I - P_S}{S} + 1$$

$$W_{convolution} = C_S{}^2 \times C \times N$$

$$B_{convolution} = N$$

I:Size of input image

C_S: Size of kernels used in the Conv layer

S: Stride of the convolution operation

P_C: Padding size; P_S: Pooling size

C: Number of channels of the input image

N: Number of Kernels

COMBINED STRUCTURE: CNN & LSTM

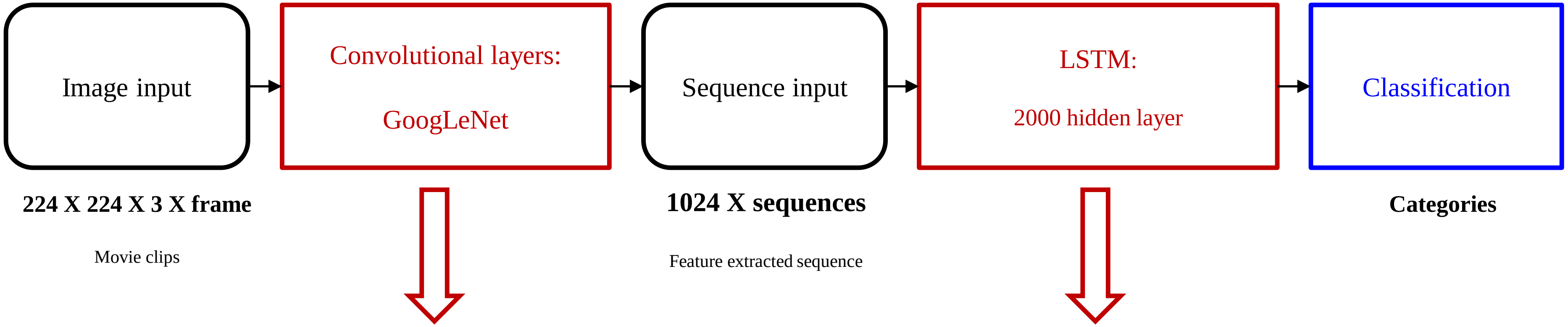

Image input

Convolutional layers:

GoogLeNet

Sequence input

LSTM:

2000 hidden layer

Classification

224 X 224 X 3 X frame

Movie clips

1024 X sequences

Feature extracted sequence

Categories

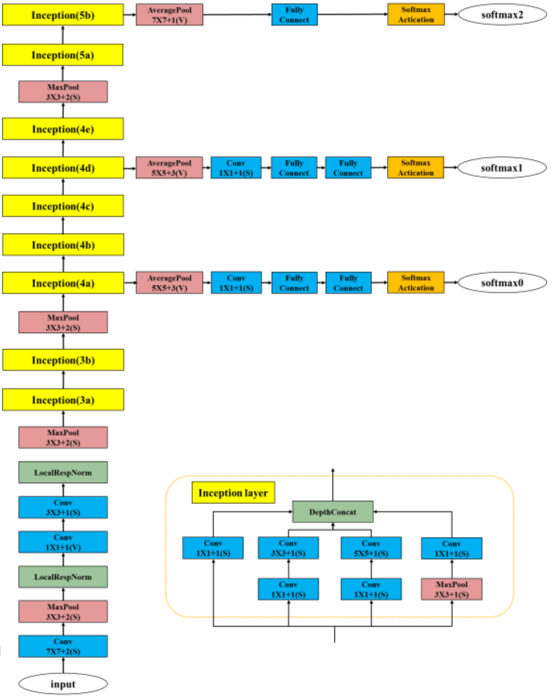

[GoogLeNet architecture, Simonyan and Zisserman(2014)]

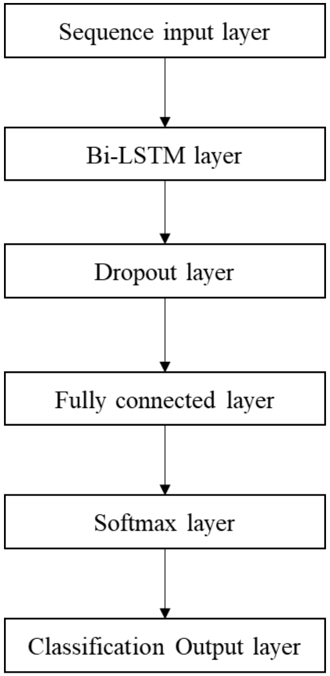

Sequence input layer

Bi-LSTM layer

Dropout layer

Fully connected layer

Softmax layer

Classification Output layer

Sequence length: 1024

Hyper-parameter

Input Size: 'auto'

Num Hidden Units: 2000

Output Mode: 'last'

State Activation Function: 'tanh'

Gate Activation Function: 'sigmoid'

Dropout probability: 0.5

Input size: auto

Output size: Number of categories

Loss function: Cross entropy loss

[LSTM network(1997)]

DATA ACQUISITION

- **Southwestern region of Jeju Island(Cha-Gui-Do)**
  - Fixed-type Wave Energy Converter / KRISO
  - with ADCP type measuring instrument

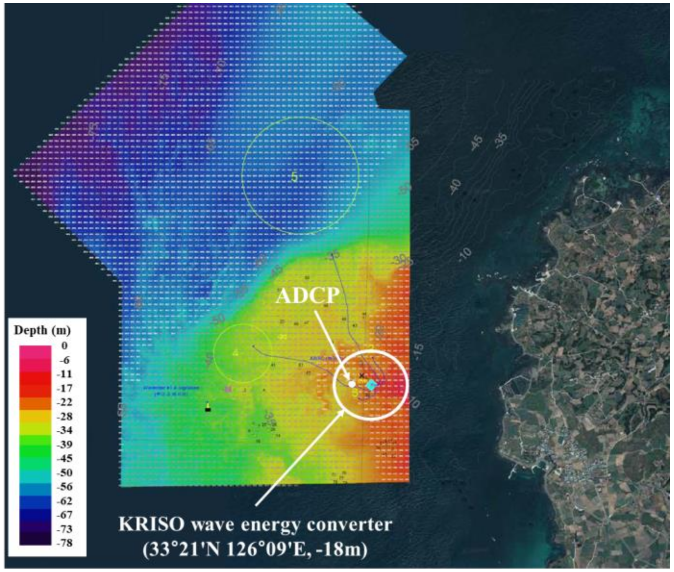

KRISO wave energy converter
(33°21'N 126°09'E, -18m)

- Maximum operating depth: 60m
- Installed depth: 18m
- Wave measuring range: -15.0 ~ +15.0m
- Period range: 1-50s

AWAC - 600 kHz

NON-PREPROCEEDED DATA

- Non-prescreened data (Sep., 2021)
  - Selecting 5 representative time durations
  - All data without any restrictions

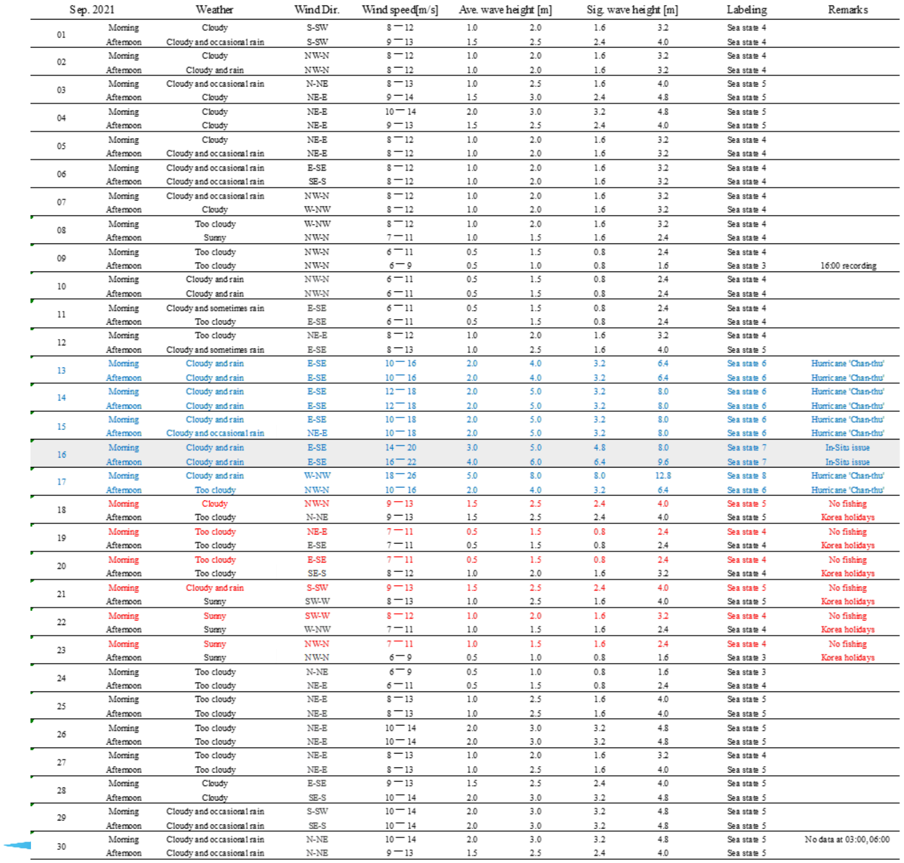

Sep. 2021		Weather	Wind Dir.	Wind speed[m/s]	Ave. wave height [m]		Sig. wave height [m]		Labeling	Remarks
01	Morning	Cloudy	S-SW	8 — 12	1.0	2.0	1.6	3.2	Sea state 4	
	Afternoon	Cloudy and occasional rain	S-SW	9 — 13	1.5	2.5	2.4	4.0	Sea state 4	
02	Morning	Cloudy	NW-N	8 — 12	1.0	2.0	1.6	3.2	Sea state 4	
	Afternoon	Cloudy and rain	NW-N	8 — 12	1.0	2.0	1.6	3.2	Sea state 4	
03	Morning	Cloudy and occasional rain	N-NE	8 — 13	1.0	2.5	1.6	4.0	Sea state 5	
	Afternoon	Cloudy	NE-E	9 — 14	1.5	3.0	2.4	4.8	Sea state 5	
04	Morning	Cloudy	NE-E	10 — 14	2.0	3.0	3.2	4.8	Sea state 5	
	Afternoon	Cloudy	NE-E	9 — 13	1.5	2.5	2.4	4.0	Sea state 5	
05	Morning	Cloudy	NE-E	8 — 12	1.0	2.0	1.6	3.2	Sea state 4	
	Afternoon	Cloudy and occasional rain	NE-E	8 — 12	1.0	2.0	1.6	3.2	Sea state 4	
06	Morning	Cloudy and occasional rain	E-SE	8 — 12	1.0	2.0	1.6	3.2	Sea state 4	
	Afternoon	Cloudy and occasional rain	SE-S	8 — 12	1.0	2.0	1.6	3.2	Sea state 4	
07	Morning	Cloudy and occasional rain	NW-N	8 — 12	1.0	2.0	1.6	3.2	Sea state 4	
	Afternoon	Cloudy	W-NW	8 — 12	1.0	2.0	1.6	3.2	Sea state 4	
08	Morning	Too cloudy	W-NW	8 — 12	1.0	2.0	1.6	3.2	Sea state 4	
	Afternoon	Sunny	NW-N	7 — 11	1.0	1.5	1.6	2.4	Sea state 4	
09	Morning	Too cloudy	NW-N	6 — 11	0.5	1.5	0.8	2.4	Sea state 4	
	Afternoon	Too cloudy	NW-N	6 — 9	0.5	1.0	0.8	1.6	Sea state 3	16:00 recording
10	Morning	Cloudy and rain	NW-N	6 — 11	0.5	1.5	0.8	2.4	Sea state 4	
	Afternoon	Cloudy and rain	NW-N	6 — 11	0.5	1.5	0.8	2.4	Sea state 4	
11	Morning	Cloudy and sometimes rain	E-SE	6 — 11	0.5	1.5	0.8	2.4	Sea state 4	
	Afternoon	Too cloudy	E-SE	6 — 11	0.5	1.5	0.8	2.4	Sea state 4	
12	Morning	Too cloudy	NE-E	8 — 12	1.0	2.0	1.6	3.2	Sea state 4	
	Afternoon	Cloudy and sometimes rain	E-SE	8 — 13	1.0	2.5	1.6	4.0	Sea state 5	
13	Morning	Cloudy and rain	E-SE	10 — 16	2.0	4.0	3.2	6.4	Sea state 6	Hurricane 'Chan-thu'
	Afternoon	Cloudy and rain	E-SE	10 — 16	2.0	4.0	3.2	6.4	Sea state 6	Hurricane 'Chan-thu'
14	Morning	Cloudy and rain	E-SE	12 — 18	2.0	5.0	3.2	8.0	Sea state 6	Hurricane 'Chan-thu'
	Afternoon	Cloudy and rain	E-SE	12 — 18	2.0	5.0	3.2	8.0	Sea state 6	Hurricane 'Chan-thu'
15	Morning	Cloudy and rain	E-SE	10 — 18	2.0	5.0	3.2	8.0	Sea state 6	Hurricane 'Chan-thu'
	Afternoon	Cloudy and occasional rain	NE-E	10 — 18	2.0	5.0	3.2	8.0	Sea state 6	Hurricane 'Chan-thu'
16	Morning	Cloudy and rain	E-SE	14 — 20	3.0	5.0	4.8	8.0	Sea state 7	In-Situ issue
	Afternoon	Cloudy and rain	E-SE	16 — 22	4.0	6.0	6.4	9.6	Sea state 7	In-Situ issue
17	Morning	Cloudy and rain	W-NW	18 — 26	5.0	8.0	8.0	12.8	Sea state 8	Hurricane 'Chan-thu'
	Afternoon	Too cloudy	NW-N	10 — 16	2.0	4.0	3.2	6.4	Sea state 6	Hurricane 'Chan-thu'
18	Morning	Cloudy	NW-N	9 — 13	1.5	2.5	2.4	4.0	Sea state 5	No fishing
	Afternoon	Too cloudy	N-NE	9 — 13	1.5	2.5	2.4	4.0	Sea state 5	Korea holidays
19	Morning	Too cloudy	NE-E	7 — 11	0.5	1.5	0.8	2.4	Sea state 4	No fishing
	Afternoon	Too cloudy	E-SE	7 — 11	0.5	1.5	0.8	2.4	Sea state 4	Korea holidays
20	Morning	Too cloudy	E-SE	7 — 11	0.5	1.5	0.8	2.4	Sea state 4	No fishing
	Afternoon	Too cloudy	SE-S	8 — 12	1.0	2.0	1.6	3.2	Sea state 4	Korea holidays
21	Morning	Cloudy and rain	S-SW	9 — 13	1.5	2.5	2.4	4.0	Sea state 5	No fishing
	Afternoon	Sunny	SW-W	8 — 13	1.0	2.5	1.6	4.0	Sea state 5	Korea holidays
22	Morning	Sunny	SW-W	8 — 12	1.0	2.0	1.6	3.2	Sea state 4	No fishing
	Afternoon	Sunny	W-NW	7 — 11	1.0	1.5	1.6	2.4	Sea state 4	Korea holidays
23	Morning	Sunny	NW-N	7 — 11	1.0	1.5	1.6	2.4	Sea state 4	No fishing
	Afternoon	Sunny	NW-N	6 — 9	0.5	1.0	0.8	1.6	Sea state 3	Korea holidays
24	Morning	Too cloudy	N-NE	6 — 9	0.5	1.0	0.8	1.6	Sea state 3	
	Afternoon	Too cloudy	NE-E	6 — 11	0.5	1.5	0.8	2.4	Sea state 4	
25	Morning	Too cloudy	NE-E	8 — 13	1.0	2.5	1.6	4.0	Sea state 5	
	Afternoon	Too cloudy	NE-E	8 — 13	1.0	2.5	1.6	4.0	Sea state 5	
26	Morning	Too cloudy	NE-E	10 — 14	2.0	3.0	3.2	4.8	Sea state 5	
	Afternoon	Too cloudy	NE-E	10 — 14	2.0	3.0	3.2	4.8	Sea state 5	
27	Morning	Too cloudy	NE-E	8 — 13	1.0	2.0	1.6	3.2	Sea state 4	
	Afternoon	Too cloudy	NE-E	8 — 13	1.0	2.5	1.6	4.0	Sea state 5	
28	Morning	Cloudy	E-SE	9 — 13	1.5	2.5	2.4	4.0	Sea state 5	
	Afternoon	Cloudy	SE-S	10 — 14	2.0	3.0	3.2	4.8	Sea state 5	
29	Morning	Cloudy and occasional rain	S-SW	10 — 14	2.0	3.0	3.2	4.8	Sea state 5	
	Afternoon	Cloudy and occasional rain	SE-S	10 — 14	2.0	3.0	3.2	4.8	Sea state 5	
30	Morning	Cloudy and occasional rain	N-NE	10 — 14	2.0	3.0	3.2	4.8	Sea state 5	No data at 03:00, 06:00
	Afternoon	Cloudy and occasional rain	N-NE	9 — 13	1.5	2.5	2.4	4.0	Sea state 5	

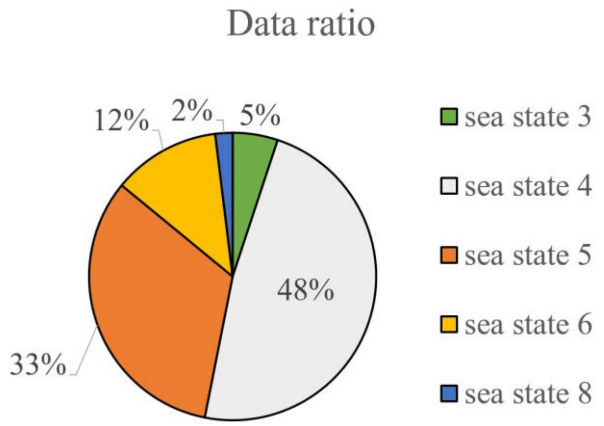


(a) Sep. 10, 2021, 18:45 ~ 18:55


(b) Sep. 21, 2021, 06:20 ~ 06:30


(c) Sep. 17, 2021, 03:00 ~ 03:05


(d) Sep. 12, 2021, 15:00 ~ 15:10


(e) Sep. 26, 2021, 15:00 ~ 15:10


(f) Sep. 17, 2021, 10:00 ~ 10:10

PRESCREENED DATA

- Well-conditioned data (May~Jul., 2020)
  - Minimized diffuse reflection of light
  - Eliminating ill-conditioned data

Date		Start time	End time	Condition	Average wave height[m]	Significant wave height[m]	Sea state
May	17	10:30	11:30	Strongly cloudy	1.25	2.00	4
	19	10:00	11:00	Strongly cloudy	3.00	4.79	6
	20	8:00	9:00	Fine	1.50	2.39	4
	24	10:00	11:00	Strongly cloudy	1.00	1.60	4
	25	10:00	11:00	Cloudy	1.00	1.60	4
	26	10:00	11:00	Cloudy	1.00	1.60	4
	28	10:00	11:00	Cloudy	1.00	1.60	4
	29	10:00	11:00	Strongly cloudy	1.00	1.60	4
	31	10:00	11:00	Cloudy & rainy	1.25	2.00	4
June	2	10:00	11:00	Fine	1.25	2.00	4
	3	10:00	11:00	Cloudy & weakly rainy	1.00	1.60	4
	4	9:00	10:00	Strongly cloudy	1.50	2.39	4
	6	10:00	11:00	Strongly cloudy	1.50	2.39	4
	7	10:00	11:00	Fine	1.25	2.00	4
	8	10:00	11:00	Fine	1.25	2.00	4
	9	10:00	11:00	Cloudy	1.50	2.39	4
	14	10:00	11:00	Cloudy	2.50	3.99	5
	15	10:00	11:00	cloudy & weakly rainy	1.50	2.39	4
	16	10:00	11:00	Cloudy	1.25	2.00	4
	19	10:00	11:00	Cloudy	2.00	3.19	5
	20	10:00	11:00	Strongly cloudy	1.50	2.39	4
	21	10:00	11:00	Fine	1.50	2.39	4
	22	8:00	9:00	Fine	1.50	2.39	4
	26	8:00	9:00	Fine	1.50	2.39	4
	28	10:00	11:00	Strongly cloudy	1.50	2.39	4
July	1	8:00	9:00	Fine	1.50	2.39	4
	4	8:00	9:00	Cloudy	1.50	2.39	4
	5	9:00	10:00	Cloudy	2.00	3.19	5
	6	8:00	9:00	Cloudy & rainy	2.00	3.19	5
	7	7:00	8:00	Cloudy & rainy	2.00	3.19	5
	8	8:00	9:00	Strongly cloudy	2.00	3.19	5
	12	8:00	9:00	Cloudy & rainy	1.50	2.39	4
	13	8:00	9:00	Cloudy & rainy	3.00	4.79	6
	14	8:00	9:00	Cloudy	3.00	4.79	6
	15	8:00	9:00	Cloudy	1.50	2.39	4
	16	8:00	9:00	Cloudy	1.00	1.60	4
	17	7:30	8:30	Fine	1.25	2.00	4

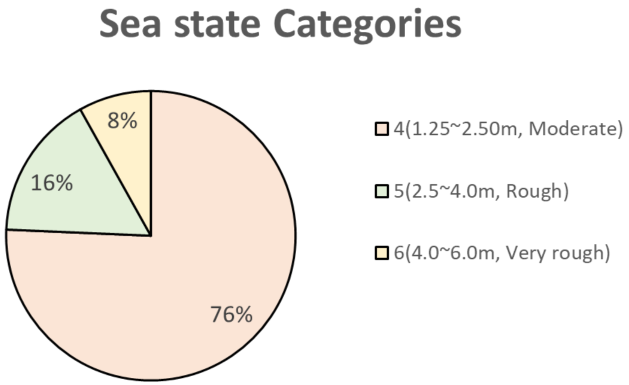

- Smallest number of data: 20,802

1. Introduction
2. Learning architecture & data acquisition
3. <u>Learning results</u>
    1. Parametric tuning
    2. Snapshot-based learning
    3. Video-based learning
4. Applications in marine engineering
5. Concluding remarks

LEARNING RESURTS - Tuning

- **Initial prediction for numerically generated short-crested waves**
  - 3 hours simulation data(0.1s sampling) → Training: 1500, Validating: 300, Testing: 300 per category
  - Only 4 hidden layers CNN

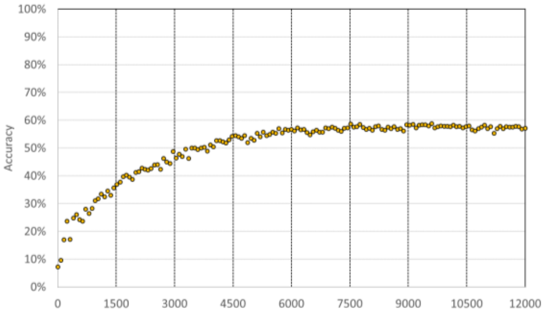

[Training accuracy]

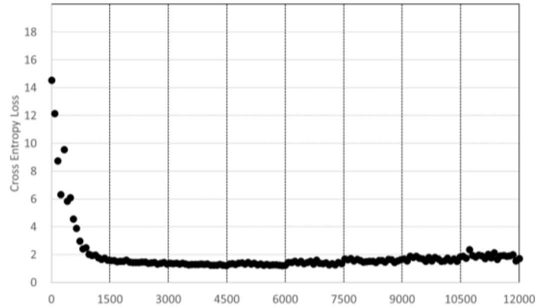

[Cross entropy loss]

	Computational Time
Image generation(CPU)	24h 26m 25s
Image classification(CPU)	33.3s
Data training(GPU)	6hr 30m 42s

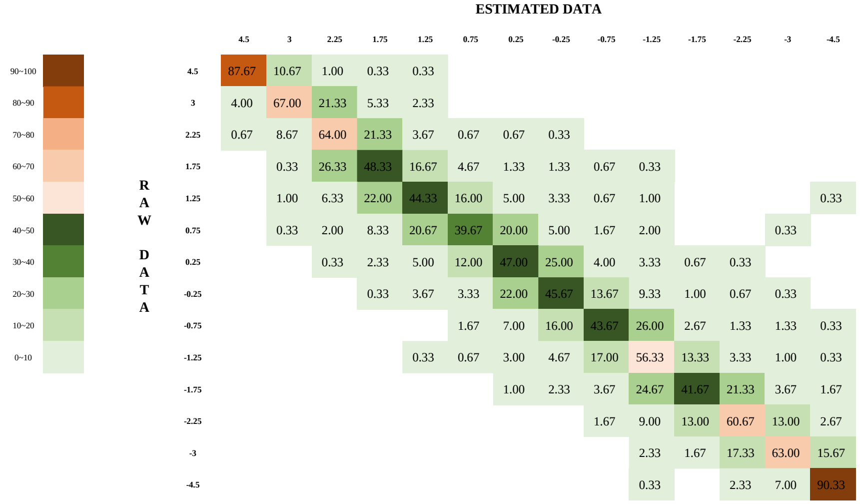

90~100	🟫
80~90	🟧
70~80	🟧
60~70	🟧
50~60	🟧
40~50	🟩
30~40	🟩
20~30	🟩
10~20	🟩
0~10	🟩

ESTIMATED DATA

RAW DATA

	4.5	3	2.25	1.75	1.25	0.75	0.25	-0.25	-0.75	-1.25	-1.75	-2.25	-3	-4.5
4.5	87.67	10.67	1.00	0.33	0.33									
3	4.00	67.00	21.33	5.33	2.33									
2.25	0.67	8.67	64.00	21.33	3.67	0.67	0.67	0.33						
1.75		0.33	26.33	48.33	16.67	4.67	1.33	1.33	0.67	0.33				
1.25		1.00	6.33	22.00	44.33	16.00	5.00	3.33	0.67	1.00				0.33
0.75		0.33	2.00	8.33	20.67	39.67	20.00	5.00	1.67	2.00			0.33	
0.25			0.33	2.33	5.00	12.00	47.00	25.00	4.00	3.33	0.67	0.33		
-0.25				0.33	3.67	3.33	22.00	45.67	13.67	9.33	1.00	0.67	0.33	
-0.75						1.67	7.00	16.00	43.67	26.00	2.67	1.33	1.33	0.33
-1.25					0.33	0.67	3.00	4.67	17.00	56.33	13.33	3.33	1.00	0.33
-1.75							1.00	2.33	3.67	24.67	41.67	21.33	3.67	1.67
-2.25									1.67	9.00	13.00	60.67	13.00	2.67
-3										2.33	1.67	17.33	63.00	15.67
-4.5										0.33		2.33	7.00	90.33

[Correlation matrix]

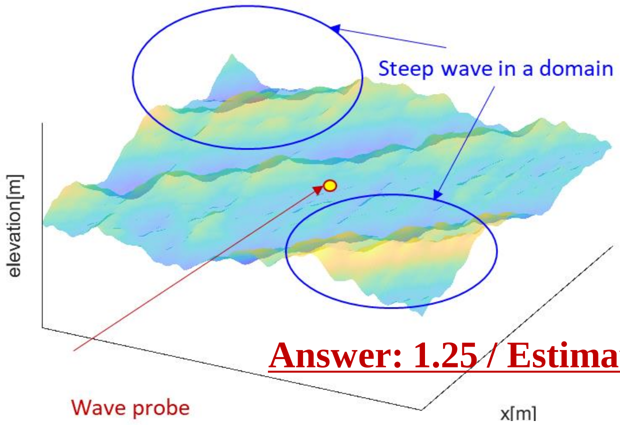

Answer: 1.25 / Estimation: -4.50

[An example of wrong prediction]

LEARNING RESURTS - Tuning

- **Hyper-parameter tuning & Data dependency check**

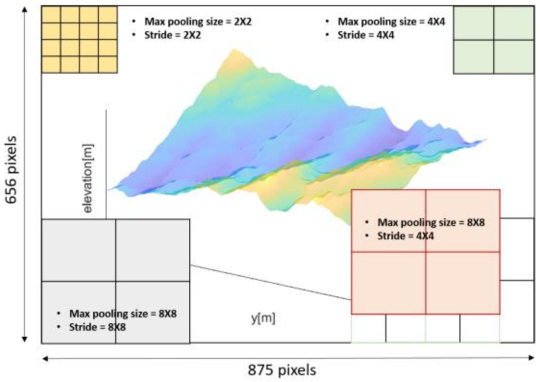

[Max-pooling size variation]

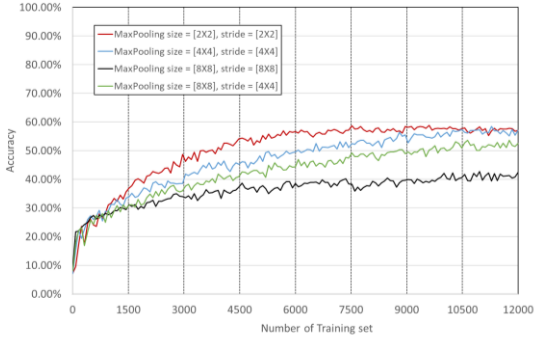

[Training accuracy]

Number of convolution layers	Filter size	Number of filters	Validation accuracy[%]	Data training time
1	3×3	32	45.62	344m 31s
2	3×3 3×3	32 64	53.07	499m 19s
3	3×3 3×3 3×3	32 64 128	56.40	380m 7s
4	3×3 3×3 3×3 3×3	32 64 128 128	57.10	390m 42s
5	3×3 3×3 3×3 3×3 3×3	32 64 128 128 128	60.52	516m 23s

[Number of convolutional layers variation]

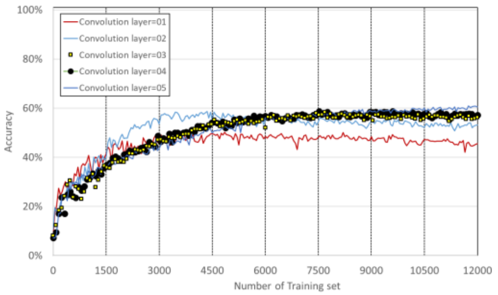

[Training accuracy]

Prediction on different dominant sea state:
Sea state 3, 5, 7

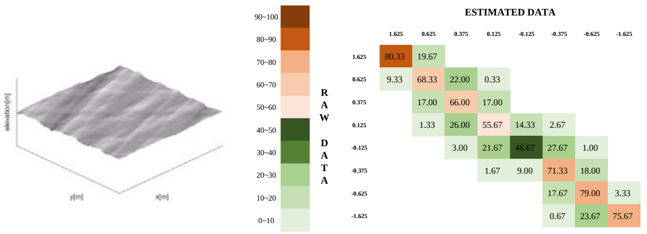

ESTIMATED DATA

	1.625	0.625	0.375	0.125	-0.125	-0.375	-0.625	-1.625
1.625	80.33	19.67						
0.625	9.33	68.33	22.00	0.33				
0.375		17.00	66.00	17.00				
0.125		1.33	26.00	55.67	14.33	2.67		
-0.125			3.00	21.67	46.67	27.67	1.00	
-0.375				1.67	9.00	71.33	18.00	
-0.625						17.67	79.00	3.33
-1.625						0.67	23.67	75.67

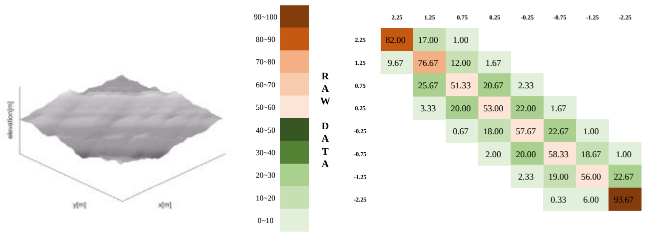

ESTIMATED DATA

	2.25	1.25	0.75	0.25	-0.25	-0.75	-1.25	-2.25
2.25	82.00	17.00	1.00					
1.25	9.67	76.67	12.00	1.67				
0.75		25.67	51.33	20.67	2.33			
0.25		3.33	20.00	53.00	22.00	1.67		
-0.25			0.67	18.00	57.67	22.67	1.00	
-0.75				2.00	20.00	58.33	18.67	1.00
-1.25					2.33	19.00	56.00	22.67
-2.25						0.33	6.00	93.67

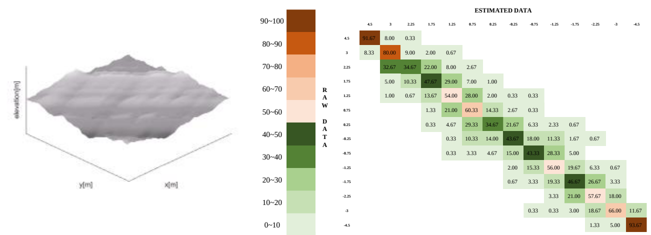

ESTIMATED DATA

	4.5	3	2.25	1.75	1.25	0.75	0.25	-0.25	-0.75	-1.25	-1.75	-2.25	-3	-4.5
4.5	91.67	8.00	0.33											
3	8.33	80.00	9.00	2.00	0.67									
2.25		32.67	34.67	22.00	8.00	2.67								
1.75		5.00	10.33	47.67	29.00	7.00	1.00							
1.25		1.00	0.67	13.67	54.00	28.00	2.00	0.33	0.33					
0.75				1.33	21.00	60.33	14.33	2.67	0.33					
0.25				0.33	4.67	29.33	34.67	21.67	6.33	2.33	0.67			
-0.25					0.33	10.33	14.00	43.67	18.00	11.33	1.67	0.67		
-0.75					0.33	3.33	4.67	15.00	43.33	28.33	5.00			
-1.25								2.00	15.33	56.00	19.67	6.33	0.67	
-1.75								0.67	3.33	19.33	46.67	26.67	3.33	
-2.25										3.33	21.00	57.67	18.00	
-3									0.33	0.33	3.00	18.67	66.00	11.67
-4.5												1.33	5.00	93.67

- Training parameters were adjusted in terms of such as max pooling size, number of convolution layers, number of trainees per category, and so on.
- Generally, accuracies per each category was not evenly high, while high accuracy was obtained for the highest and lowest categories that characterize the ocean environment.

LEARNING RESURTS – Snapshot-based learning

- **Learning results with non-prescreened data**
  - Prediction on sea state

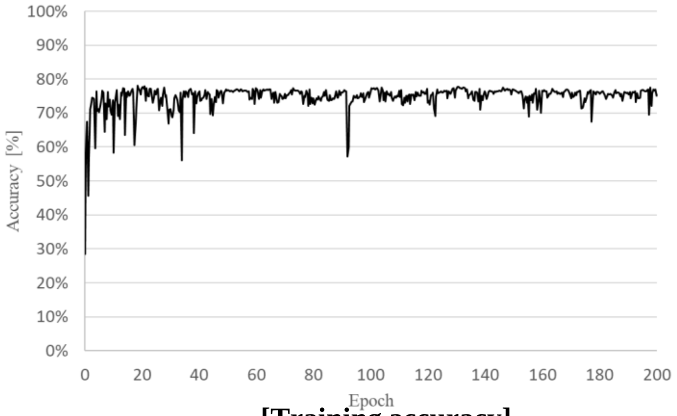

[Training accuracy]

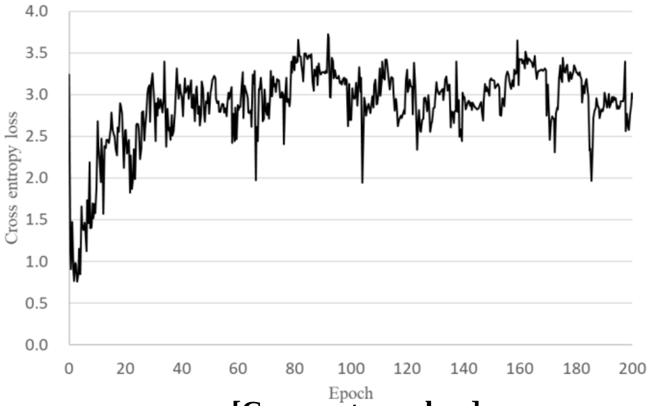

[Cross entropy loss]

	SS3 (predicted)	SS4 (predicted)	SS5 (predicted)	SS6 (predicted)	SS8 (predicted)
SS3 (observed)	99.996%	0.004%	0.000%	0.000%	0.000%
SS4 (observed)	36.953%	11.416%	51.607%	0.024%	0.000%
SS5 (observed)	0.661%	21.785%	76.239%	0.000%	1.315%
SS6 (observed)	0.000%	34.719%	4.066%	0.016%	61.198%
SS8 (observed)	0.000%	0.000%	0.000%	0.001%	99.999%

[Correlation matrix]

LEARNING RESURTS – Snapshot-based learning

- **Learning results with non-prescreened data**
  - Applicability evaluation with deformed images

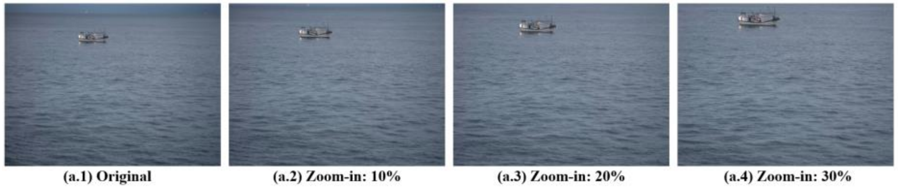

(a.1) Original (a.2) Zoom-in: 10% (a.3) Zoom-in: 20% (a.4) Zoom-in: 30%

	Original	10% zoom-in	20% zoom-in	30% zoom-in
SS3	1.000	0.861	0.284	0.166
SS5	0.762	0.674	0.573	0.481
SS8	1.000	0.998	0.880	0.651

[Image distortion: focusing- considering surge motion]

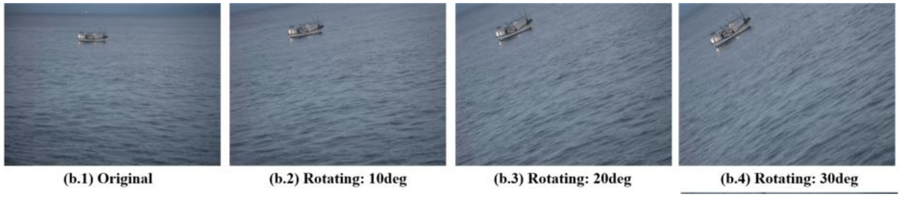

(b.1) Original (b.2) Rotating: 10deg (b.3) Rotating: 20deg (b.4) Rotating: 30deg

	Original	10% rotating	20% rotating	30% rotating
SS3	1.000	0.327	0.248	0.126
SS5	0.762	0.341	0.229	0.184
SS8	1.000	0.550	0.493	0.479

[Image distortion: rotating - considering roll motion]

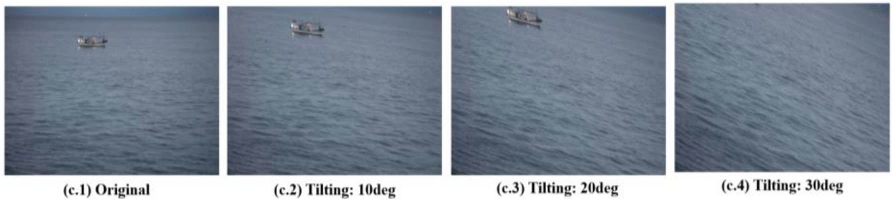

(c.1) Original (c.2) Tilting: 10deg (c.3) Tilting: 20deg (c.4) Tilting: 30deg

	Original	10% tilting	20% tilting	30% tilting
SS3	1.000	0.099	0.009	0.000
SS5	0.762	0.497	0.382	0.286
SS8	1.000	0.740	0.674	0.483

[Image distortion: tilting - considering roll & pitch motion]

LEARNING RESURTS – Snapshot-based learning

- **Learning results with non-prescreened data**
  - Trial for increasing prediction performance: angle detection and re-rotation

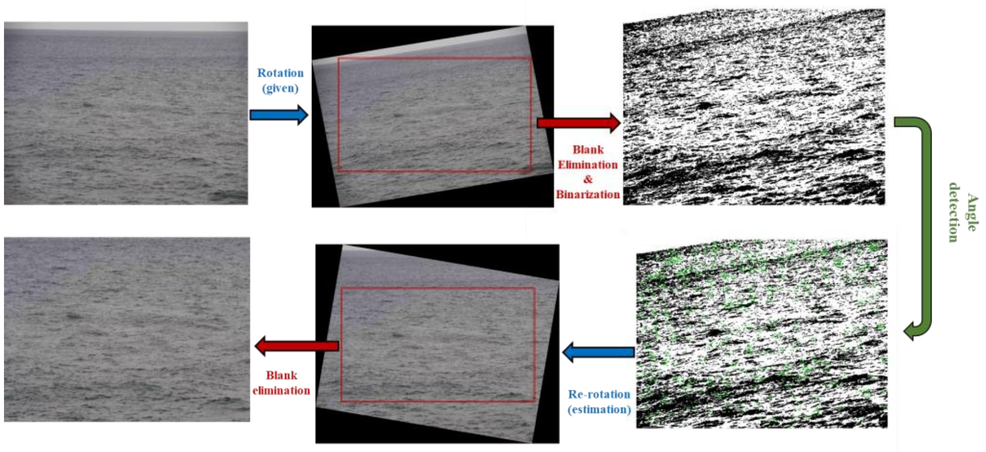

[Image re-rotation process]

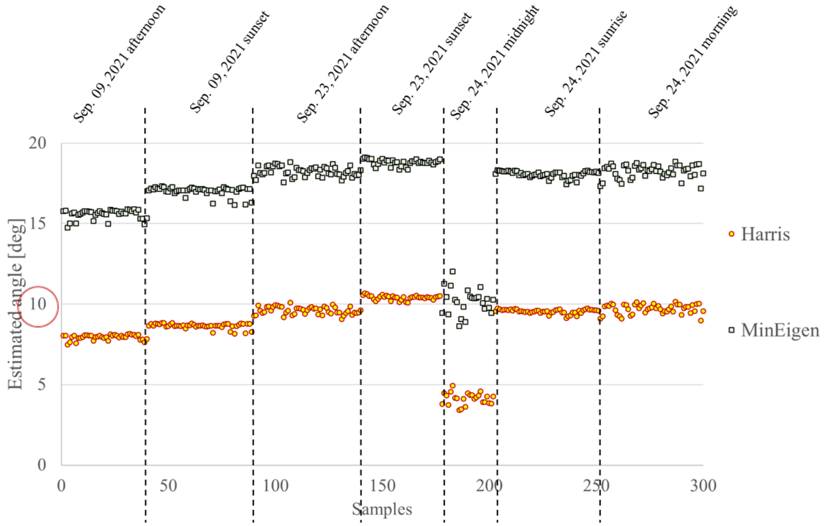

[Detected angles for 10deg pre-rotated data in sea state 03]

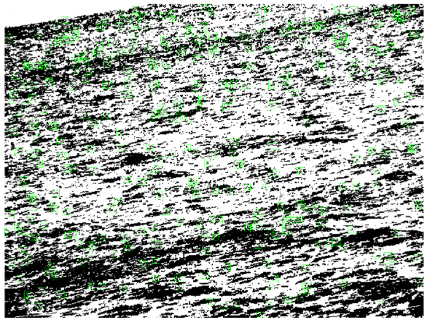

[Harris (Harris C. and M. Stephens, 1988)]

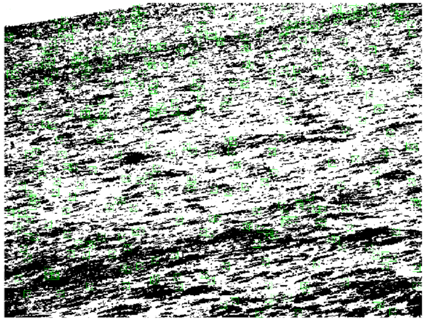

[Minimum Eigenvalue (Shi J. and C. Tomasi, 1994)]

- Applying feature tracking algorithm
- **Harris method: Classical method with auto-correlation detector**

LEARNING RESURTS – Snapshot-based learning

- **Learning results with non-prescreened data**
  - Prediction results for the trial with angle detection and re-rotation

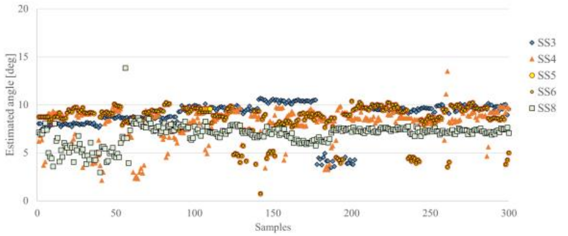

[Estimated angle with Harris method with 10deg rotated images]

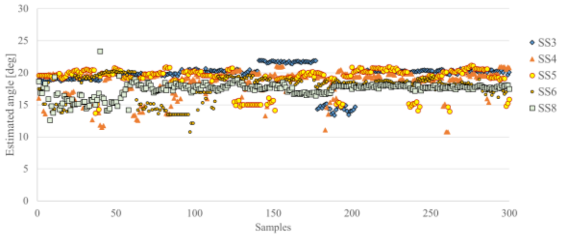

[Estimated angle with Harris method with 20deg rotated images]

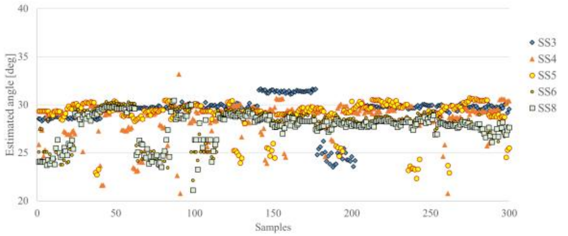

[Estimated angle with Harris method with 30deg rotated images]

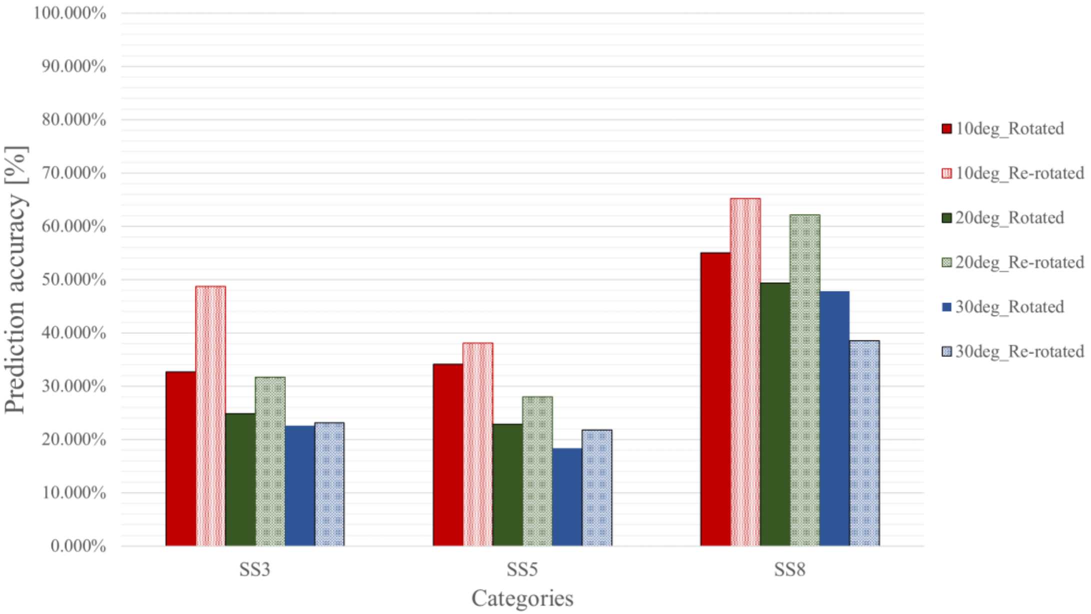

[Comparison between predictions with rotated and re-rotated images]

- Relatively well estimation on angles
- Prediction performance is generally increased in small rotated angles
- In harsh environment, estimation performance is rather poor at large angle.
- Image loss due to continuous rotations is considered as the main cause

LEARNING RESURTS – Snapshot-based learning

- **Learning results with prescreened data**
  - Initial learning of **sea state** prediction
  - Only CNN applied

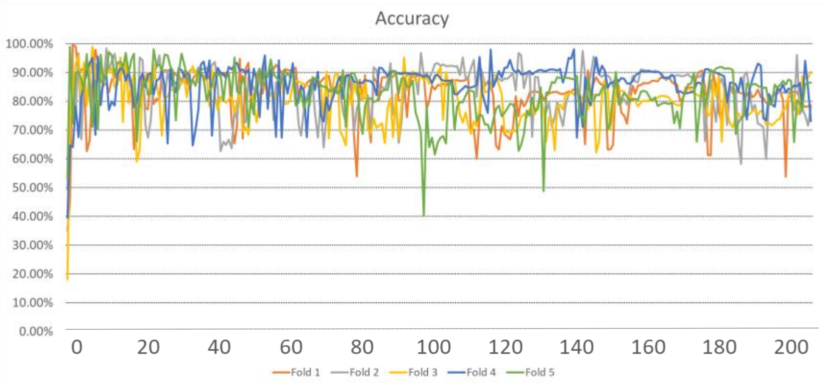

[Global training accuracy of validating data]

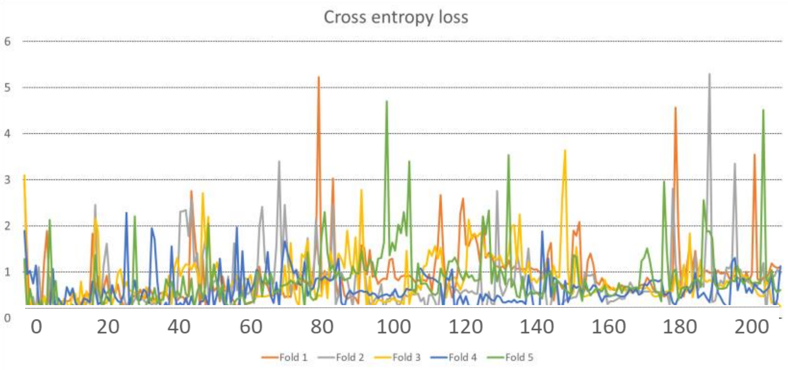

[Cross entropy loss of validating data]

		Sea state 4 (observed)	Sea state 5 (observed)	Sea state 6 (observed)
Sea state 4 (predicted)	fold 1	0.989	0.011	0.000
	fold 2	0.715	0.285	0.000
	fold 3	1.000	0.000	0.000
	fold 4	0.997	0.003	0.000
	fold 5	1.000	0.000	0.000
Sea state 5 (predicted)	fold 1	0.998	0.002	0.000
	fold 2	0.734	0.266	0.000
	fold 3	0.533	0.467	0.000
	fold 4	0.648	0.352	0.000
	fold 5	0.949	0.051	0.000
Sea state 6 (predicted)	fold 1	0.000	0.000	1.000
	fold 2	0.000	0.000	1.000
	fold 3	0.000	0.000	1.000
	fold 4	0.000	0.000	1.000
	fold 5	0.000	0.001	0.999

[Prediction probability of testing data]

- Relatively good prediction performance
  - Remarkably high prediction in sea state 6
  - Prediction confusion between sea state 4 and sea state 5

LEARNING RESURTS – Snapshot-based learning

- **Learning results with prescreened data**
  - Initial learning of **average wave height** prediction
  - Only CNN applied

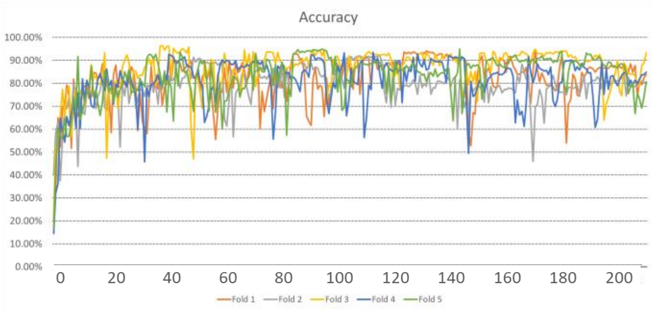

[Global training accuracy of validating data]

	H,ave=1.00m (predicted)	H,ave=1.25m (predicted)	H,ave=1.50m (predicted)	H,ave=2.00m (predicted)	H,ave=2.50m (predicted)	H,ave=3.00m (predicted)
H,ave=1.00m (observed)	0.04%	3.73%	**96.23%**	0.00%	0.00%	0.00%
H,ave=1.25m (observed)	0.88%	**77.64%**	4.15%	17.33%	0.00%	0.00%
H,ave=1.50m (observed)	14.11%	0.00%	**65.89%**	15.34%	4.50%	0.15%
H,ave=2.00m (observed)	0.00%	0.29%	**55.40%**	44.30%	0.02%	0.00%
H,ave=2.50m (observed)	0.00%	0.00%	1.02%	0.00%	**98.98%**	0.00%
H,ave=3.00m (observed)	0.00%	0.00%	0.00%	0.00%	0.00%	**100.00%**

[Prediction probability of testing data]

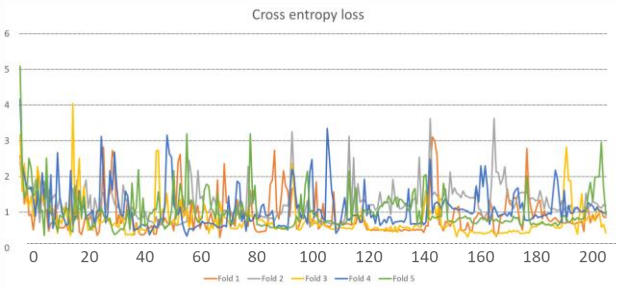

[Cross entropy loss of validating data]

		Actual answer	
		TRUE	FALSE
Classification result	TRUE	TP 64.474%	FP 30.741%
	FALSE	FN 35.525%	TN 69.259%

$$(precision) = \frac{TP}{TP+FP} = 67.714\%$$

$$(Recall) = \frac{TP}{TP+FN} = 64.475\%$$

$$(Accuracy) = \frac{TP+TN}{TP+FN+FP+TN} = 66.867\%$$

[Confusion matrix for average wave height classification with snapshots]

KAIST

INTERIM REMARKS

- **Training parameters were adjusted in terms of such as max pooling size, number of convolution layers, number of trainees per category, and so on.**
- **Generally, accuracies per each category was not evenly high, while high accuracy was obtained for the highest and lowest categories that characterize the ocean environment.**
- **When performing prediction on the non-prescreened data of the real sea, the accuracy did not exceed 80% and was stagnant.**
- **With the present network and simple image processing techniques, it is difficult to apply to the problem of deformed images.**
- **In predictions with prescreened snapshots, the prediction was made relatively well, but there was some confusion among small wave regions.**

LEARNING RESURTS – Video-based learning

- **Preparation of videos**
    - 2Hz for videos
    - Average wave height prediction
    - Combined learning scheme

      (GoogLeNet & bi-LSTM)

		# of training data		# of validating data		# of testing data	
Movie clip I (Length=6s)	H,ave=1.00m	2596	81.00%	288	9.00%	320	10.00%
	H,ave=1.25m	3229	81.00%	359	9.00%	398	10.00%
	H,ave=1.50m	6431	81.00%	715	9.00%	794	10.00%
	H,ave=2.00m	2320	81.00%	258	9.00%	286	10.00%
	H,ave=2.50m	485	81.10%	54	9.00%	59	9.90%
	H,ave=3.00m	1404	81.00%	156	9.00%	173	10.00%
Movie clip II (Length=30s)	H,ave=1.00m	518	81.00%	58	9.00%	64	10.00%
	H,ave=1.25m	646	81.10%	72	9.00%	79	9.90%
	H,ave=1.50m	1287	81.00%	143	9.00%	158	9.90%
	H,ave=2.00m	464	81.00%	52	9.00%	57	10.00%
	H,ave=2.50m	97	81.70%	11	9.10%	11	9.20%
	H,ave=3.00m	281	81.20%	31	9.00%	34	9.80%
Movie clip III (Length=60s)	H,ave=1.00m	259	81.00%	29	9.00%	32	10.00%
	H,ave=1.25m	323	81.20%	36	9.00%	39	9.80%
	H,ave=1.50m	644	81.00%	72	9.00%	79	9.90%
	H,ave=2.00m	232	81.20%	26	9.00%	28	9.80%
	H,ave=2.50m	49	82.40%	5	9.20%	5	8.50%
	H,ave=3.00m	140	81.20%	16	9.00%	17	9.80%
Movie clip IV (Length=180s)	H,ave=1.00m	86	81.50%	10	9.10%	10	9.40%
	H,ave=1.25m	107	81.10%	12	9.00%	13	9.80%
	H,ave=1.50m	214	81.10%	24	9.00%	26	9.80%
	H,ave=2.00m	77	81.50%	9	9.10%	9	9.50%
	H,ave=2.50m	16	85.30%	2	9.50%	1	5.30%
	H,ave=3.00m	47	82.10%	5	9.10%	5	8.80%
Movie clip V (Length=300s)	H,ave=1.00m	52	81.60%	6	9.10%	6	9.40%
	H,ave=1.25m	64	80.90%	7	9.00%	8	10.10%
	H,ave=1.50m	129	81.50%	14	9.10%	15	9.50%
	H,ave=2.00m	47	82.10%	5	9.10%	5	8.80%
	H,ave=2.50m	8	73.60%	1	8.20%	2	18.20%
	H,ave=3.00m	27	79.40%	3	8.80%	4	11.80%

[Video clip conversion]

[H,ave=1.00m]

[H,ave=2.00m]

[H,ave=1.25m]

[H,ave=2.50m]

[H,ave=1.50m]

[H,ave=3.00m]

LEARNING RESURTS – Video-based learning

- **Learning results with prescreened data**
  - Prediction results

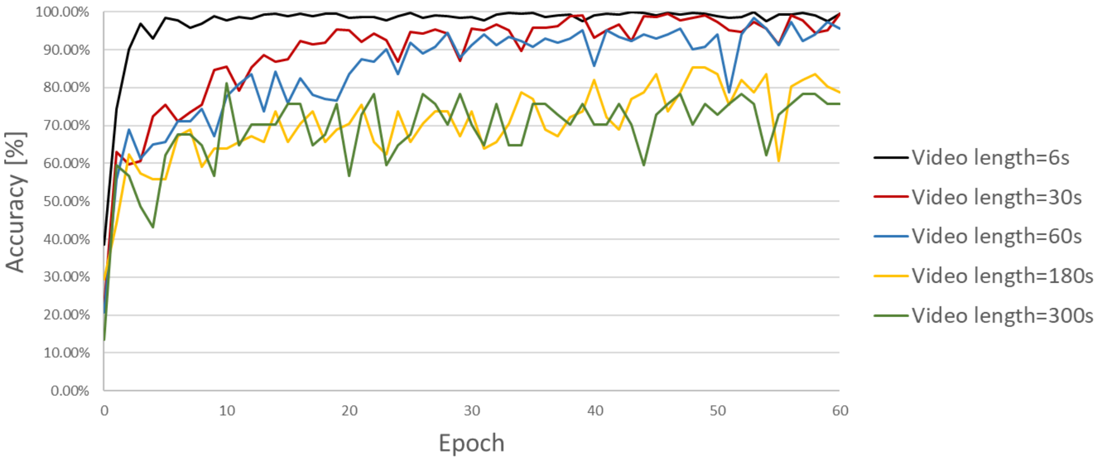

[Global accuracy]

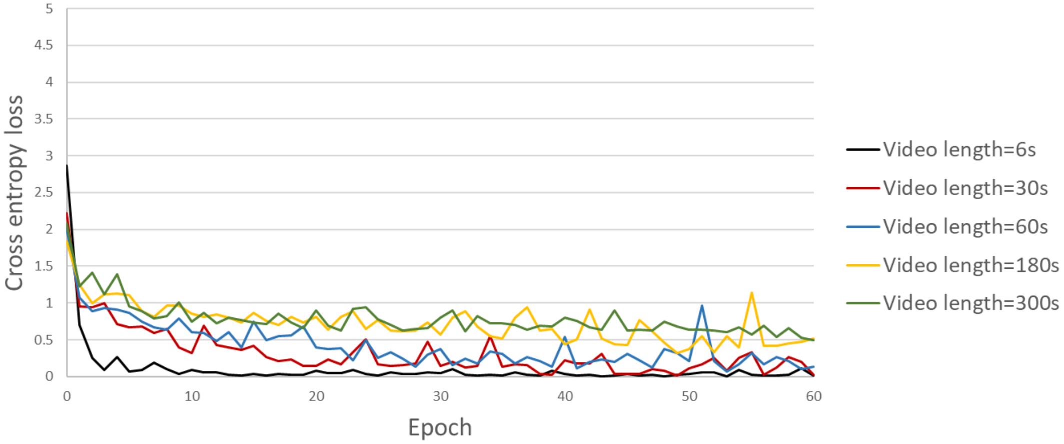

[Cross entropy loss]

LEARNING RESURTS – Video-based learning

- **Learning results with prescreened data**

	H,ave 1.00m (predicted)	H,ave 1.25m (predicted)	H,ave 1.50m (predicted)	H,ave 2.00m (predicted)	H,ave 2.50m (predicted)	H,ave 3.00m (predicted)
H,ave 1.00m (observed)	21.01%	0.80%	78.10%	0.08%	0.00%	0.00%
H,ave 1.25m (observed)	0.00%	3.62%	95.84%	0.53%	0.00%	0.00%
H,ave 1.50m (observed)	0.83%	3.85%	75.62%	17.35%	2.24%	0.11%
H,ave 2.00m (observed)	0.00%	0.01%	4.75%	95.23%	0.01%	0.00%
H,ave 2.50m (observed)	0.00%	0.00%	0.03%	0.00%	99.96%	0.00%
H,ave 3.00m (observed)	0.00%	0.00%	2.02%	0.00%	0.00%	97.97%

[Correlation matrix with 6s videos]

	H,ave 1.00m (predicted)	H,ave 1.25m (predicted)	H,ave 1.50m (predicted)	H,ave 2.00m (predicted)	H,ave 2.50m (predicted)	H,ave 3.00m (predicted)
H,ave 1.00m (observed)	1.62%	79.39%	18.98%	0.01%	0.00%	0.00%
H,ave 1.25m (observed)	0.00%	1.32%	98.66%	0.01%	0.00%	0.00%
H,ave 1.50m (observed)	0.01%	3.68%	88.26%	1.02%	7.01%	0.01%
H,ave 2.00m (observed)	0.00%	0.19%	70.38%	26.52%	2.90%	0.00%
H,ave 2.50m (observed)	0.00%	0.16%	0.47%	0.01%	99.35%	0.01%
H,ave 3.00m (observed)	0.00%	0.00%	0.01%	0.00%	0.00%	99.99%

[Correlation matrix with 30s videos]

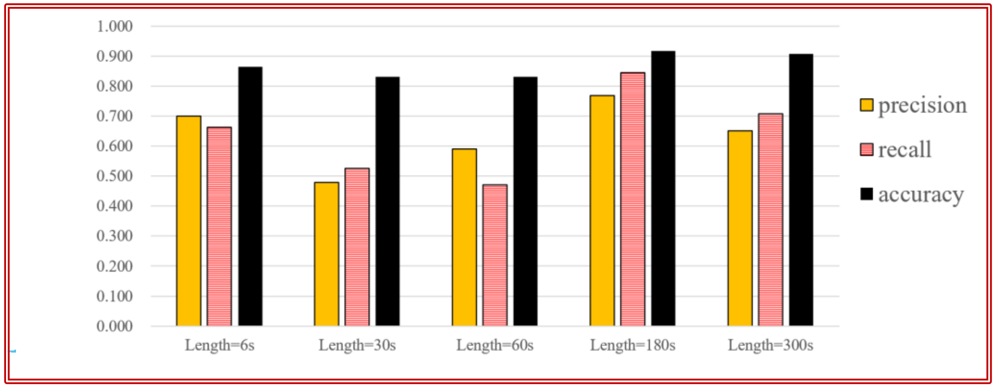

	H,ave 1.00m (predicted)	H,ave 1.25m (predicted)	H,ave 1.50m (predicted)	H,ave 2.00m (predicted)	H,ave 2.50m (predicted)	H,ave 3.00m (predicted)
H,ave 1.00m (observed)	0.95%	93.46%	5.49%	0.05%	0.05%	0.01%
H,ave 1.25m (observed)	0.00%	0.31%	99.55%	0.12%	0.01%	0.00%
H,ave 1.50m (observed)	0.16%	20.01%	79.44%	0.31%	0.05%	0.03%
H,ave 2.00m (observed)	0.01%	1.03%	31.82%	66.91%	0.22%	0.00%
H,ave 2.50m (observed)	0.00%	0.01%	57.27%	0.04%	42.65%	0.03%
H,ave 3.00m (observed)	0.00%	0.00%	0.02%	0.00%	0.00%	99.98%

[Correlation matrix with 60s videos]

	H,ave 1.00m (predicted)	H,ave 1.25m (predicted)	H,ave 1.50m (predicted)	H,ave 2.00m (predicted)	H,ave 2.50m (predicted)	H,ave 3.00m (predicted)
H,ave 1.00m (observed)	77.69%	14.34%	0.88%	7.03%	0.06%	0.00%
H,ave 1.25m (observed)	1.50%	75.33%	3.43%	18.71%	1.03%	0.00%
H,ave 1.50m (observed)	0.45%	15.62%	58.54%	23.00%	2.12%	0.27%
H,ave 2.00m (observed)	0.19%	1.59%	1.86%	84.67%	11.69%	0.00%
H,ave 2.50m (observed)	0.00%	0.00%	0.07%	0.08%	99.84%	0.00%
H,ave 3.00m (observed)	0.00%	0.00%	0.11%	0.00%	0.00%	99.89%

[Correlation matrix with 180s videos]

	H,ave 1.00m (predicted)	H,ave 1.25m (predicted)	H,ave 1.50m (predicted)	H,ave 2.00m (predicted)	H,ave 2.50m (predicted)	H,ave 3.00m (predicted)
H,ave 1.00m (observed)	73.80%	18.18%	6.76%	0.43%	0.81%	0.02%
H,ave 1.25m (observed)	0.91%	60.63%	29.74%	8.34%	0.36%	0.01%
H,ave 1.50m (observed)	1.00%	20.02%	66.35%	7.90%	1.13%	3.60%
H,ave 2.00m (observed)	1.08%	36.58%	15.68%	45.87%	0.77%	0.02%
H,ave 2.50m (observed)	0.87%	9.87%	39.95%	23.60%	25.55%	0.16%
H,ave 3.00m (observed)	0.00%	0.00%	7.85%	0.03%	0.01%	92.11%

[Correlation matrix with 300s videos]

LEARNING RESURTS – Video-based learning

- **Prescreened data preparation**
  - Prediction with 180s videos
  - Data augmentation for 'Have=2.50m'
    - Splitting the screen
  - Height interval = 0.5m
    - Eliminating of 'Have=1.25m'

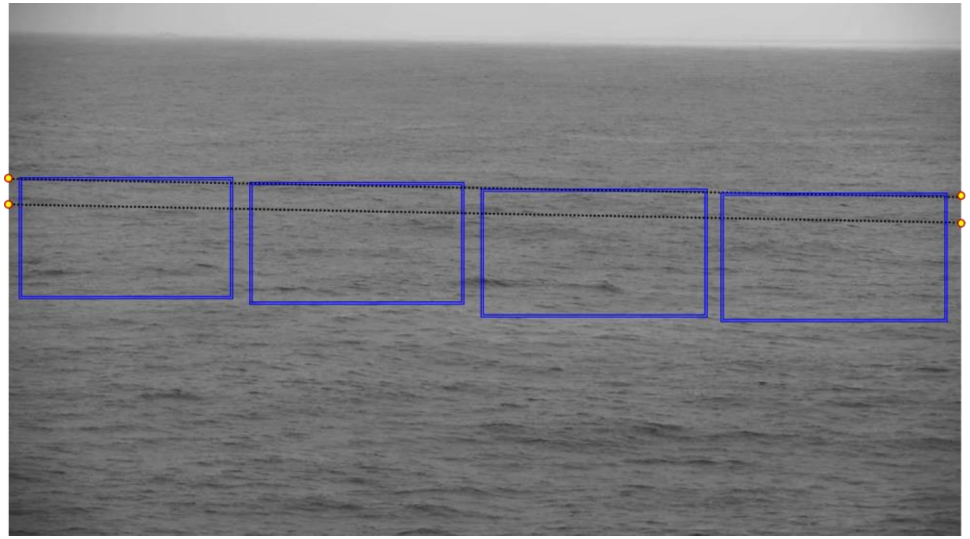

[Data augmentation for 'Have=2.50m' category]

		# of training data		# of validating data		# of testing data	
Movie clip (180s, 360frames)	H,ave=1.00m	86	81.1%	10	9.4%	10	9.4%
	H,ave=1.50m	214	81.1%	24	9.1%	26	9.8%
	H,ave=2.00m	77	81.1%	9	9.5%	9	9.5%
	H,ave=2.50m	**62(+46)**	**81.6%**	**7(+5)**	**9.2%**	**7(+6)**	**9.2%**
	H,ave=3.00m	47	82.1%	5	8.8%	5	8.8%

[Data classification with augmentation in 'Have=2.50m' category]

LEARNING RESURTS – Video-based learning

- **Learning results with prescreened data**

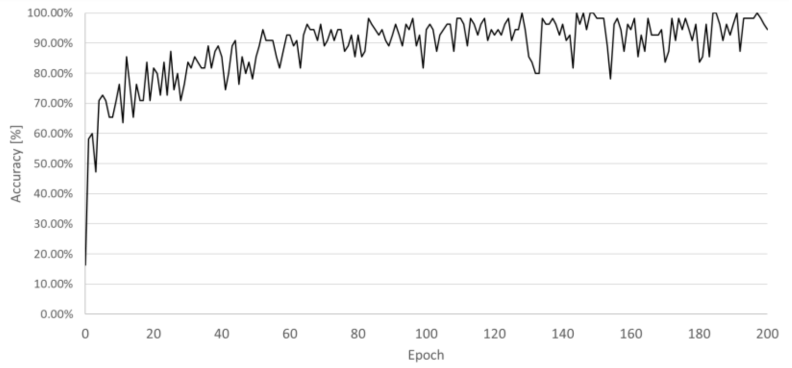

[Global accuracy]

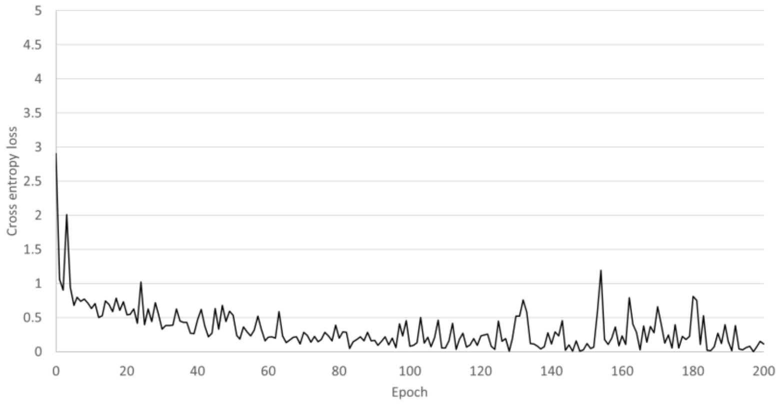

[Cross entropy loss]

[Correlation matrix]

	H,ave 1.00m (predicted)	H,ave 1.50m (predicted)	H,ave 2.00m (predicted)	H,ave 2.50m (predicted)	H,ave 3.00m (predicted)
H,ave 1.00m (observed)	99.95%	0.00%	0.04%	0.00%	0.00%
H,ave 1.50m (observed)	4.24%	80.11%	15.32%	0.04%	0.29%
H,ave 2.00m (observed)	11.02%	0.29%	88.65%	0.05%	0.00%
H,ave 2.50m (observed)	0.00%	0.47%	0.09%	99.44%	0.00%
H,ave 3.00m (observed)	0.00%	1.93%	0.00%	0.00%	98.07%

LEARNING RESURTS – Video-based learning

- **Comprehensive comparisons**

	Precision	Recall	Accuracy
Snapshot-based learning	0.677	0.645	0.669
Video-based learning	0.769	0.846	0.917
Video-based learning (0.5 intervals and augmentation)	0.932	0.969	0.972

[Comparison in machine learning methods]

	Operation difficulty	Equipment expense	O/M expense	Preparation time to measure	accuracy	Coverage area	Ease of access
Non-contact measurement (LiDAR, radar)	△	△	△	△	▲	△	△/▽
In-situ measurement (resistance, capacitance, ultrasonic)	△	△	△	△	▲	△/▽	▽
Satellite measurement	▲	▲	▲	▲	△	▲	△
Optical image based measurement (by vision analysis)	▽	▽	▼	▽	△	▽	▽
Optical image based measurement (by machine learning)	▽	▽	▼	▲	△	▽	▲

▲	High/long
△	Intermediate
▽	Low/short
▼	negligible

[Comparison in machine learning methods]

INTERIM REMARKS

- The combined deep learning model with CNN and LSTM was applied to the average wave height classification based on video-type data.
- The suitable video length was evaluated.
- In the small wave area, classification at 0.25m intervals was difficult, and the accuracy was also poor in the category with a small number of data.
- Setting the equal height interval of 0.5m and augmentation of insufficient data increased the prediction performance significantly.

APPLICATIONS IN MARINE ENGINEERING

https://www.index.go.kr/potal/main/EachDtlPageDetail.do?idx_cd=2855
https://coast.mof.go.kr/coastScene/coastMediaService.do
http://www.kcg.go.kr/

Forecasting Status in Korea

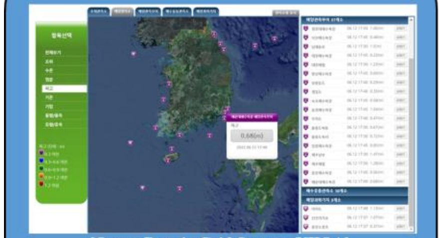

[Ocean Data in Grid System, KHOA]

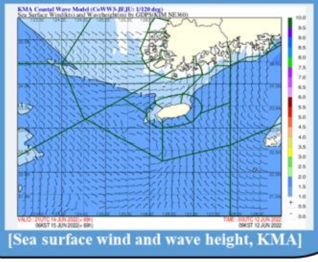

[Sea surface wind and wave height, KMA]

Numerous CCTV along coastal lines

Numerous CCTV along coastal lines

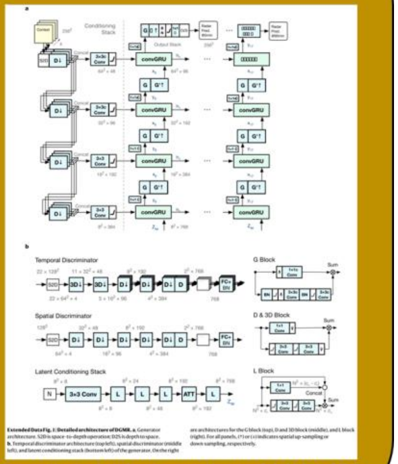

[Nowcasting using deep generative model(2021), UK]

Less precise, but
in-situ real-time now-casting

Utilizing
existing cameras

Newly developing
networks

National marine now-casting map

- **Estimation sea states of Korea’s representative oceans with snapshots**
  - Evaluating of possibility of establishing a national marine now-casting map using the developed system
    1. Initially, data acquisition by research infrastructures
    2. Constructing the train network with advanced deep learning technology
    3. Application of the developed system to major ports and beaches

APPLICATIONS IN MARINE ENGINEERING

- **Research infrastructures**

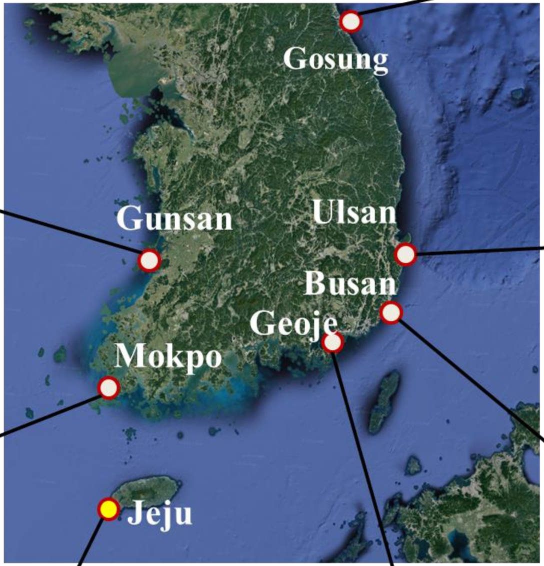

Seawater Energy Plant Research Center

Surveying vessel

Autonomous navigating Research Center

Marine Testbed

KIOST Research Vessel Deepwater Research Center

Wave energy converter

Offshore Research Center

APPLICATIONS IN MARINE ENGINEERING

- **Feasibility study on ship application**
  1. Development of a camera using gimbal to compensate the ship rotational motions
  2. Coupled supervising ship motions and optical images
  3. Long-term data acquisition

- **Snapshot images from ship-mounted camera(3rd Aug. 2021)**
  - Mokpo coastal car-ferry: DreamIsland
    - 449G/T, 11 knots, 14 miles(1hr 50m)
  - Sea state: 2 (Hs=0.1~0.2m)

Shin-An	Wind			Ambient pressure [hPa]	Humidity [%]	Temperature, air [°C]	Temperature, water [°C]	Wave				
Weather casting buoy	Dir.	Speed [m/s]	Gust [m/s]					Max. height[m]	**Sig. height [m]**	Ave. height [m]	Period[s]	Dir.
13:30 3rd Aug. 2021	SE	5	6.9	1007.3	77	27.8	25.3	0.2	**0.1**	0.1	2.7	NS
14:00 3rd Aug. 2021	SSE	3.4	5.6	1007.4	77	27.9	25.3	0.2	**0.1**	0.1	2.3	SSE
14:30 3rd Aug. 2021	S	1.6	3.9	1007.7	79	27.6	25.5	0.3	**0.1**	0.1	3	WNW
15:00 3rd Aug. 2021	SSW	2.7	3.9	1007.8	85	26.7	25.8	0.4	**0.2**	0.1	2.3	NE
15:30 3rd Aug. 2021	SSW	3.6	4.8	1007.5	80	27.3	25.9	0.4	**0.1**	0	2.3	NNW

APPLICATIONS IN MARINE ENGINEERING

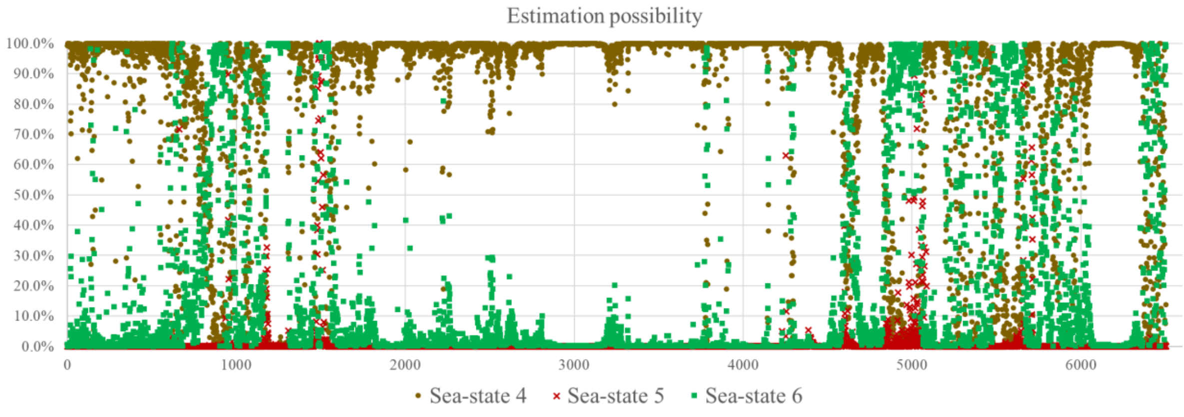

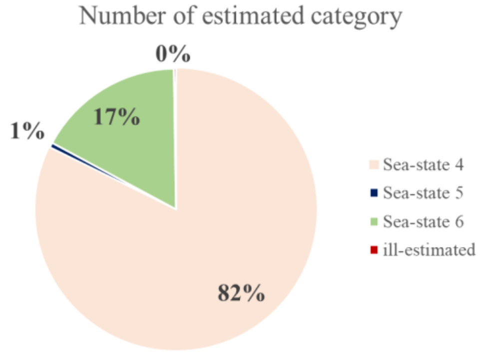

	Sea-state 4 (n=5350)		Sea-state 5 (n=37)		Sea-state 6 (n=1100)		ill-predicted (n=16)	
	Mean	STD	Mean	STD	Mean	STD	Mean	STD
Sea-state 4	**94.99%**	0.098	6.22%	0.121	14.52%	0.153	35.38%	0.104
Sea-state 5	0.10%	0.012	**83.38%**	0.157	1.26%	0.049	25.86%	0.153
Sea-state 6	4.91%	0.097	10.40%	0.120	**84.23%**	0.155	38.76%	0.102

sea-state 4 estimated

sea-state 6 estimated

ill-estimated

CONCLUDING REMARKS

- Deep learning technology was adopted to estimate the sea conditions through optical image and the constructed method was applied to a real problem.
- Suitability of this approach was checked with numerical wave snapshots.
- Using non-prescreened data, we confirmed that the CNN-based deep learning with snapshots has a certain limitation in classifying the sea conditions.
- Some image processing techniques were applied to increase the prediction accuracy, but the effect is insignificant.
- The combined deep learning model(CNN and LSTM) was then applied. It showed a good prediction performance with data augmentation and data rearrangement.
- Few scenarios were suggested in marine engineering for utilizing these machine learning technology.
- Further studies should be conducted for training and predicting with longer-term data, applied to navigating ships.

Thank you
for
your attention!

REFERENCES

[01] van Rijn, L.C., 2007. Manual sediment transport measurements in rivers, estuaries and coastal seas - Chapter 12, in: Measuring Instruments for Fluid Velocity, Pressure and Wave Height. Aquapublications, Netherlands.

[02] Korea Meteorological Administrator, 2020, KMA business introduction on marine observation, https://web.kma.go.kr/eng/biz/observation_07.jsp.

[03] Korea Hydrographic and Oceanographic Agency, 2020. Ocean data in grid framework (Korean website), http://www.khoa.go.kr/oceangrid/khoa/koofs.do.

[04] Jahne, B., Klinke, J., Waas, S., 1994. Imaging of short ocean wind waves: A critical theoretical review. J. Opt. Soc. Am. A: Opt., Image Sci., and Vis. 11(8), 2197–2209. https://doi.org/10.1364/JOSAA.11.002197.

[05] Chou, C.R., Yim, J.Z., Huang, W.P., 2004. Determining the hydrographic parameters of the surface of water from the image sequences of a CCD camera. Exp. Fluids. 36, 515–527. https://doi.org/10.1007/s00348-003-0664-3.

[06] Viriyakijja, K., Chinnarasri, C., 2015. Wave flume measurement using image analysis. Acquat. Proced. 4, 522–531. https://doi.org/10.1016/j.aqpro.2015.02.068.

[07] Piepmeier, J., Waters, J., Broussard, R., 2006. 2006-2364: A stereo vision-based wave surface measurement project. 2006 Annual Conference & Exposition, Chicago, USA. DOI: 10.18260/1-2—1332.

[08] McCulloch, W.S., Pitts, W., 1943. A logical calculus of the ideas immanent in nervous activity. Bull. Math. Biophys. 5, 115–133.

[09] Rosenblatt, F., 1958. The perception: A probabilistic model for information storage and organization in the brain. Psychol. 386.

[10] Rumelhart, D.E., Hinton, G.E., Williams, R.J., 1986. Learning representations by back-propagating errors. Nature. 323, 533–536.

[11] Hinton, G.E., Osindero, S., Teh, Y.W., 2006. A fast learning algorithm for deep belief nets. Neural Comput. 18, 1527–1554.

[12] Alex, K., Ilya, S., Geoffrey, E.H., 2012. ImageNet classification with deep convolutional neural networks. Proceedings of the 25th International Conference on Neural Information Processing Systems, Lake Tahoe, NV, USA, 1097–1105.

[13] Silver, D., Huang, A., Maddison, C.J., Guez, A., Sifre, L., van den Driessche, G., Schrittwieser, J., Antonoglou, I., Panneershelvam, V., Lanctot, M., Dieleman, S., Grewe, D., Nham, J., Kalchbrenner, N., Sutskever, I., Lillicrap, T., Leach, M., Kavukcuoglu, K., Graepel, T., Hassabis, D., 2016. Mastering the game of Go with deep neural networks and tree search. Nature. 529, 484.

[14] Silver, D., Schrittwieser, J., Simonyan, K., Antonoglou, I., Huang, A., Guez, A., Hubert, T., Baker, L., Lai, M., Bolton, A., Chen, Y., Lillicrap, T., Hui, F., Sifre, L., Van den Driessche, G., Graepel, T., Hassabis, D., 2017. Mastering the game of Go without human knowledge. Nature. 550, 354.

[15] LeCun, Y., Bengio, Y., Hinton, G., 2015. Deep learning. Nature. 521, 436–444.

[16] Deo, M.C., 2010. Artificial neural networks in coastal and ocean engineering. Ind. J. of Geo-Mar. Sci. 39(4), 589–596. http://nopr.niscair.res.in/handle/123456789/10807.

[17] Kutz, J.N., 2017. Deep learning in fluid dynamics. J. Fluid Mech. 814, 1–4. https://doi.org/10.1017/jfm.2016.803.

[18] Sclavounos, P.D., Ma, Y., 2018. Artificial intelligence machine learning in marine hydrodynamics. Proceedings of the ASME 2018 37th International Conference on Ocean, Offshore and Arctic Engineering, Madrid, Spain, OMAE2018-77599. https://doi.org/10.1115/OMAE2018-77599.

[19] Ahmad, H., 2019. Machine learning applications in oceanography. Aquat. Res. 2(3), 161–169. https://doi.org/10.3153/AR19014.

[20] Ramirez, W.A., Leong, Z.Q., Nguyen, H.D., Jayasinghe, S.G., 2020. Machine learning post processing of underwater vehicle pressure sensor array for speed measurement. Ocean Eng. 213, 107771, 1–6. https://doi.org/10.1016/j.oceaneng.2020.107771.

[21] Gheliotis, M., Lazakis, I., Theotokatos, G., 2020. Machine learning and data-driven fault detection for ship systems operations. Ocean Eng. 216, 107968, 1–17. https://doi.org/10.1016/j.oceaneng.2020.107968.

[22] Berghout, T., Mouss, L.H., Bentrcia, T., Elbouchikhi, E., 2021. A deep supervised learning approach for condition-based maintenance of naval propulsion systems. Ocean Eng. 221, 108525, 1–11. https://doi.org/10.1016/j.oceaneng.2020.108525.

[23] Zamani, A., Solomatine, D., Azimian, A., Heemink, A., 2008. Learning from data for wind-wave forecasting. Ocean Eng. 35, 953–962. https://doi.org/10.1016/j.oceaneng. 2008.03.007.

[24] Mahjoobi, J., Mosabbel, E.A., 2009. Prediction of significant wave height using regressive support vector machines. Ocean Eng. 36, 339–347. https://doi.org/ 10.1016/j.oceaneng.2009.01.001.

[25] Wei, C.C., 2017. Nearshore wave prediction using data mining techniques during typhoons: A case study near Taiwan’s northeastern coast. Energ. 11(1), 11. https://doi.org/10.3390/en11010011.

[26] James, S.C., Zhang, Y., O’Donncha, F., 2018. A machine learning framework to forecast wave conditions. Coast. Eng. 137, 1–10. https://doi.org/10.1016/j.coastaleng. 2018.03.004.

[27] Sarkar, D., Osborne, M.A., Adcock, T.A.A., 2018. Prediction of tidal currents using Bayesian machine learning. Ocean Eng. 158, 221–231. https://doi.org/10.1016/j.oceaneng.2018.03.007.

[28] Stringari, G.E., Harris, D.L., Power, H.E., 2019. A novel machine learning algorithm for tracking remotely sensed waves in the surf zone. Coast. Eng. 147, 149–158. https://doi.org/10.1016/j.coastaleng.2019.02.002.

[29] Kim, S., Tom, T.H.A., Takeda, M., Mase, H., 2021. A framework for transformation to nearshore wave from global wave data using machine learning techniques: Validation at the Port of Hitachinaka, Japan. Ocean Eng. 221, 108516, 1–13. https://doi.org/10.1016/j.oceaneng.2020.108516.

[30] Demetriou, D., Michailides, C., Papanastasiou, G., Onoufriou, T., 2021. Coastal zone significant wave height prediction by supervised machine learning classification algorithms. Ocean Eng. 221, 108592, 1–15. https://doi.org/10.1016/j.oceaneng.2021. 108592.

[31] Zhong, G., Liu, B., Guo, Y., and Miao, H., 2018. Sea State Bias Estimation with Least Absolute Shrinkage and Selection Operator (LASSO). J. Ocean Univ. China. 17(5), 1019–1025. https://doi.org/10.1017/s11802-018-3572-0.

REFERENCES

[32] Zhong, G., Qu, J., Wang, H., Liu, B., Jiao, W., Fan, Z., Miao, H., and Hedjam, R., 2020. Trace-Norm Regularized Multi-Task Learning for Sea State Bias Estimation. J. Ocean Univ. China. 19(6), 1292-1298. https://doi.org/10.1017/s11802-020-4267-x.

[33] Liu, T., Zhang, Y., Qi, L., Dong, J., Lv, M., Wen, Q., 2019. WaveNet: learning to predict wave height and period from accelerometer data using convolutional neural network. Proceedings of International Conference on Environment and Ocean Engineering, Xiamen, China. https://doi.org/10.1088/1755-1315/369/1/012001.

[34] Buscombe, D., Carini, R.J., 2019. A data-driven approach to classifying wave breaking in infrared imagery. Remote Sens. 11(7), 859. https://doi.org/10.3390/rs11070859.

[35] Masoumi, M., 2021. Ocean data classification using unsupervised machine learning: Planning for hybrid wave-wind offshore energy devices. Ocean Eng. 219, 108387, 1–15. https://doi.org/10.1016/j.oceaneng.2020.108387.

[36] Demetriou, D., Michailides, C., Papanastasiou, G., Onoufriouu, T., 2021. Coastal zone significant wave height prediction by supervised machine learning classification algorithms. Ocean Eng. 221, 108592, 1-15.

[37] Ravuri, S., Lenc, K., Willson, M., Kangin, D., Lam, R., Mirowski, P., Fitzsimons, M., Athanassiadou, M., Kashem, S., Madge, S., Prudden, R., Mandhane, A., Clark, A., Brock, A., Simonyan, K., Hadsell, R., Robinson, N., Clandy, E., Arribas, A., Mohamed, S., 2021. Skilful precipitation nowcasting using deep generative models of radar. Nature. 597, 672-677.

[38] Ewans, K., Feld, G., Jonathan, P., 2014. On wave radar measurement. Ocean Dynamics. 64(9), 1281–303.

[39] Simonyan, K., Zisserman, A., 2014. Very deep convolutional networks for large-scale image recognition. arXiv, arXiv:1409.1556.

[40] He, K., Zhang, X., Ren, S., Sun, J., 2016. Deep residual learning for image recognition. Proceedings of the 2016 IEEE Conference on Computer Vision and Pattern Recognition (CVPR), Las Vegas, NV, USA, 770–778.

[41] Szegedy, C., Liu, W., Jia, Y., Sermanet, P., Reed, S., Anguelov, D., Erhan, D., Vanhoucke, V., Rabinovich., 2014. Going Deeper with Convolutions. arXiv, arXiv:1409.4842v1.

[42] Szegedy, C., Vanhoucke, V., Ioffe, S., Shlens, J., Wojna, Z., 2016. Rethinking the inception architecture for computer vision. Proceedings of the 2016 IEEE Conference on Computer Vision and Pattern Recognition (CVPR), Las Vegas, NV, USA, 2818–2826.

[43] Chollet, F., 2017. Xception: Deep learning with depthwise separable convolutions. Proceedings of the 2017 IEEE Conference on Computer Vision and Pattern Recognition (CVPR), Honolulu, HI, USA, 1251–1258.

[44] Szegedy, C., Ioffe, S., Vanhoucke, V., Alemi, A.A., 2017. Inception-v4, Inception-ResNet and the impact of residual connections on learning. Proceedings of the Thirty-First AAAI Conference on Artificial Intelligence, San Francisco, CA, USA, 4278–4284.

[45] Sandler, M., Howard, A., Zhu, M., Zhmoginov, A., Chen, L.C., 2018. MobileNetV2: Inverted residuals and linear bottlenecks. Proceedings of the IEEE Conference on Computer Vision and Pattern Recognition (CVPR), pp. 4510–4520.

[46] Beale, M.H., Hagan, M.T., Demuth, H.B., 2020. Deep Learning ToolboxTM User’s Guide. MathWorks, Natick, MA, USA, https://kr.mathworks.com/help/deeplearning/.

[47] Hochreiter, S., Schmidhuber, J., 1997. Long Short-Term Memory. Neural Computation. 9(8), 1735-1780. http://www.bioinf.jku.at/publications/older/2604.pdf.

[48] Gers, F.A., Schmidhuber, J., 2000. Recurrent nets that time and cost. Proceedings of the IEEE-INNS-ENNS International Joint Conference on Neural Networks, Como, Italy, 6697377. DOI: 10.1109/IJCNN.2000.861302.

[49] Cho, K., Bahdanau, D., Bougares, F., Schwenk, H., Bengio, Y., 2014. Learning Phrase Representations using RNN Encoder-Decoder for Statistical Machine Translation. arXiv, arXiv:1406.1078v3.

[50] Yao, K., Cohn, T., Vylomova, K., Duh, K., Dyer, C., 2015. Depth-Gated Recurrent Neural Networks. arXiv, arXiv:1508.03790v2.

[51] Koutnik, J., Greff, K., Gomez, F., Schmidhuber, J., 2014. A Clockwork RNN. arXiv, arXiv:1402.3511v1.

[52] DNVGL, 2019. DNVGL Recommended Practice: Environmental Conditions and Environmental Loads. DNVGL-RP-C205, Oslo, Norway, https://oilgas.standards.dnvgl.com/download/dnvgl-rp-c205-environmental-conditions-and-environmental-loads.

[53] International Towing Tank Conference, 2012. ITTC – Recommended Procedures and Guidelines: Speed and Power Trials, Part 1 Preparation and Conduct. 7.5-04-01-01.1, https://ittc.info/media/4208/75-04-01-011.pdf.

[54] Johnson, J.M. and Khoshgoftaar, T.M., 2019. Survey on deep learning with class imbalance. Journal of Big Data. 6:27, 1-54. https://doi.org/10/1186/s40537-019-0192-5.

[55] Leutenegger, S., Chli, M., Siegwart, R.Y., 2011. BRISK: Binary Robust invariant scalagle keypoints. Proceedings of the 2011 International Conference on Computer Vison, Barcelona, Spain, https://doi.org/10.1109/ICCV.2011.6126542.

[56] Rosten, F. and Drummond, T., 2005. Fusing points and lines for high performance tracking. The 10th IEEE International Conference on Computer Vision. 2. 1508-1515.

[57] Harris, C. and Stephens, M., 1988. A Combined Corner and Edge Detector. Proceedings of the 4th Alvey Vision Conference, Manchester, UK, 147-151.

[58] Alcantarilla, P.F., Bartoli, A., Davison, A.J., 2012. KAZE Features. In: Fitzgibbon, A., Lazebnik, S., Perona, P., Sato, Y., Schmid, C. (eds) Computer Vision – ECCV 2012. ECCV 2012. Lecture Notes in Computer Science, vol 7577. Springer, Berlin, Heidelberg. https://doi.org/10.1007/978-3-642-33783-3_16.

[59] Shi, J. and Tomasi, C., 1994. Good Features to Track. IEEE Conference on Computer Vision and Pattern Recognition(CVPR94), Seattle, Washington, USA, 593-600.

[60] Rublee, E., Rabaud, V., Konolige, K., Bradski, G. 2011. ORB: An Efficient Alternative to SIFT or SURF. Proceedings of the 2011 International Conference on Computer Vison, Barcelona, Spain, 2564-2571.

[61] Bay, H., ESS, H., Tuytelaars, T., van Gool, L. 2008. SURF: Speeded Up Robust Features. Computer Vision and Image Understanding(CVIU). 110(3). 346-359.

Appendix. Ocean env. measuring in Korea

Source: Korea Hydrographic and Oceanographic Agency
http://www.khoa.go.kr/oceangrid/khoa/koofs.do
Korea Meteorological Administration

• Ocean Environment Observation Methodologies and Status of South Korea

Type	Figures
Ocean Data Buoy	
Light House AWS	
Wave Radar	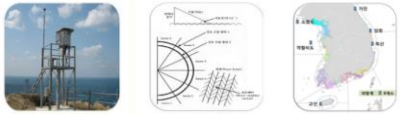
Coastal Wave Buoy	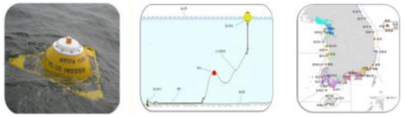
Drifting Buoy	
Coastal Long Wave Monitoring System	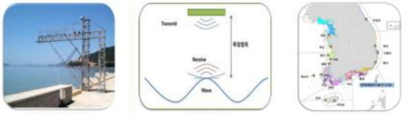
Port Weather Monitoring System	
Ship Weather Monitoring System	

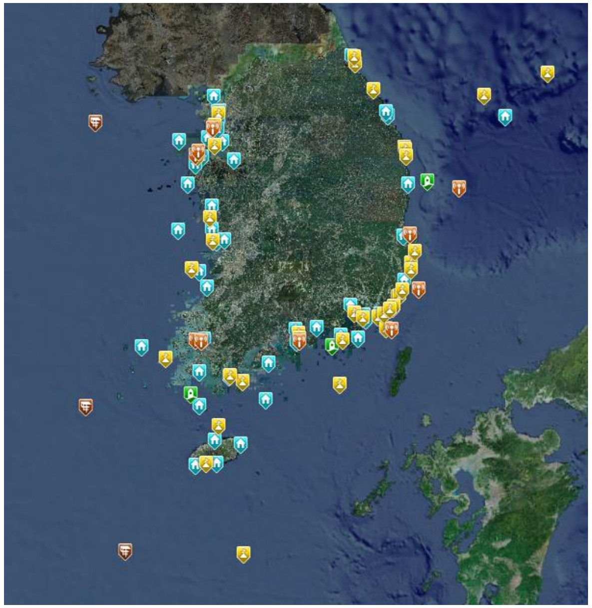

- **48 tidal observations**
- **3 ocean observations**
- **37 observation buoys**
- **10 current observations**
- **3 ocean scientific stations**

- **Easily accessible and relatively high accuracy**
- **However, numerous accidents of coastal ship are exist.**
  - **Inaccurate forecasting, Unpredictable radical change**
- **More high resolution marine map and rigorous ship operation management have been still important.**

Appendix. History of neural network

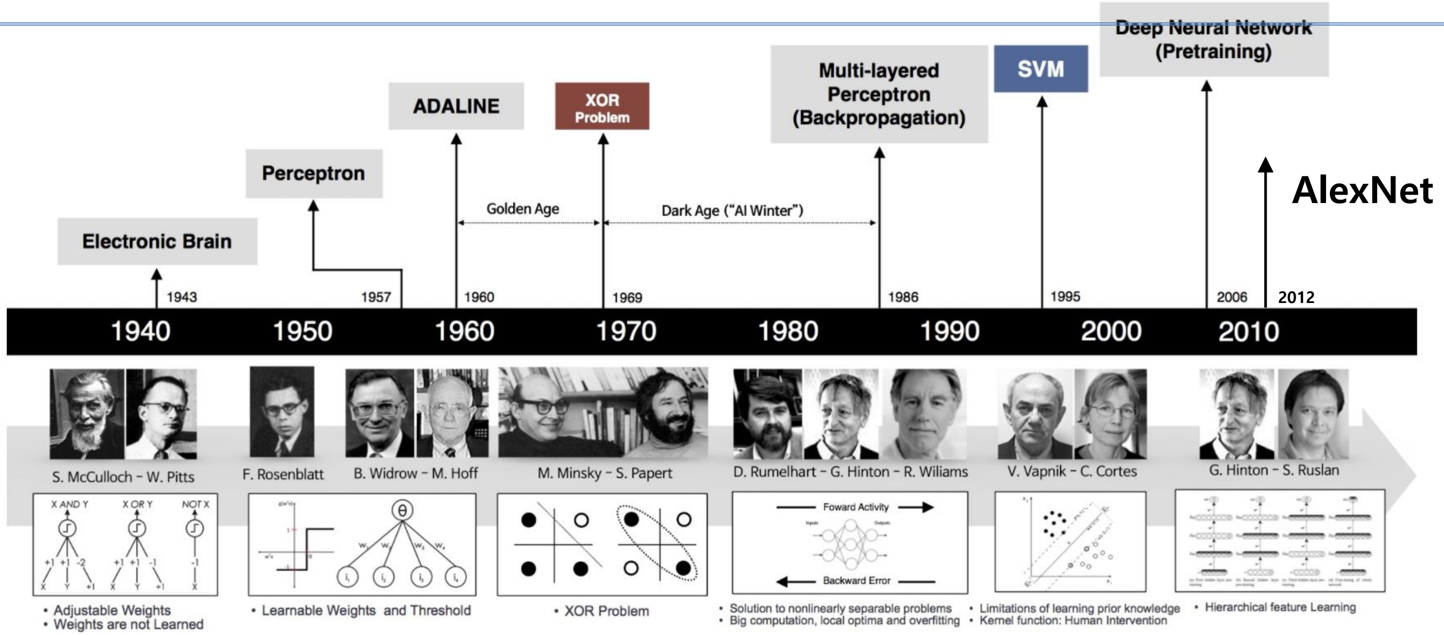

1940s - The beginning of Neural Networks (Electronic Brain)

1950s and 1960s - The first golden age of Neural Networks (Perceptron)

1970s - The winter of Neural Networks (XOR problem)

1980s - Renewed enthusiasm (Multilayered Perceptron, backpropagation)

1990s - Subfield of Radial Basis Function Networks was developed

2000s - The power of Neural Networks Ensembles & Support Vector Machines is apparent

2006 - Hinton presents the Deep Belief Network (DBN)

2009 - Deep Recurrent Neural Network

2010 - Convolutional Deep Belief Network (CDBN)

2011 - Max-Pooling CDBN

2012 - ILSVRC(ImageNet Large Scale Visual Recognition Challenge) winner using CNN

ReLU, dropout, overlapping pooling, local response normalization, data augmentation

2016 – AlphaG0 issue

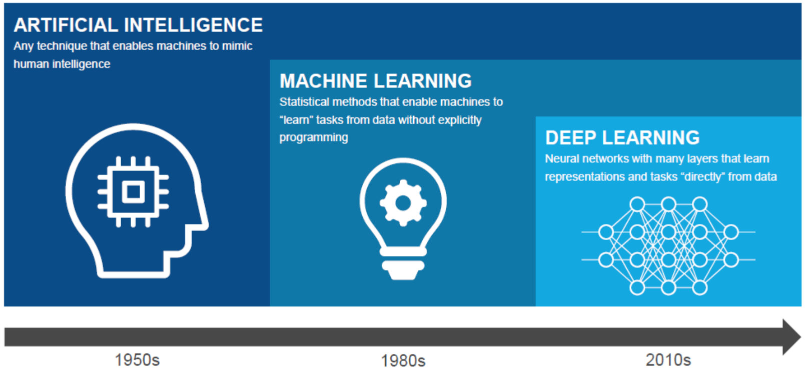

Source: Deepkapha.ai

Appendix. Sea scale

- ## Douglas Sea Scale

Degree	Hs [m]	Description
0	-	Calm (Glassy)
1	0~0.10	Calm (rippled)
2	0.10~0.50	Smooth
3	0.50~1.25	Slight
4	1.25~2.50	Moderate
5	2.50~4.00	Rough
6	4.00~6.00	Very rough
7	6.00~9.00	High
8	9.00~14.00	Very high
9	14.00~	Phenomenal

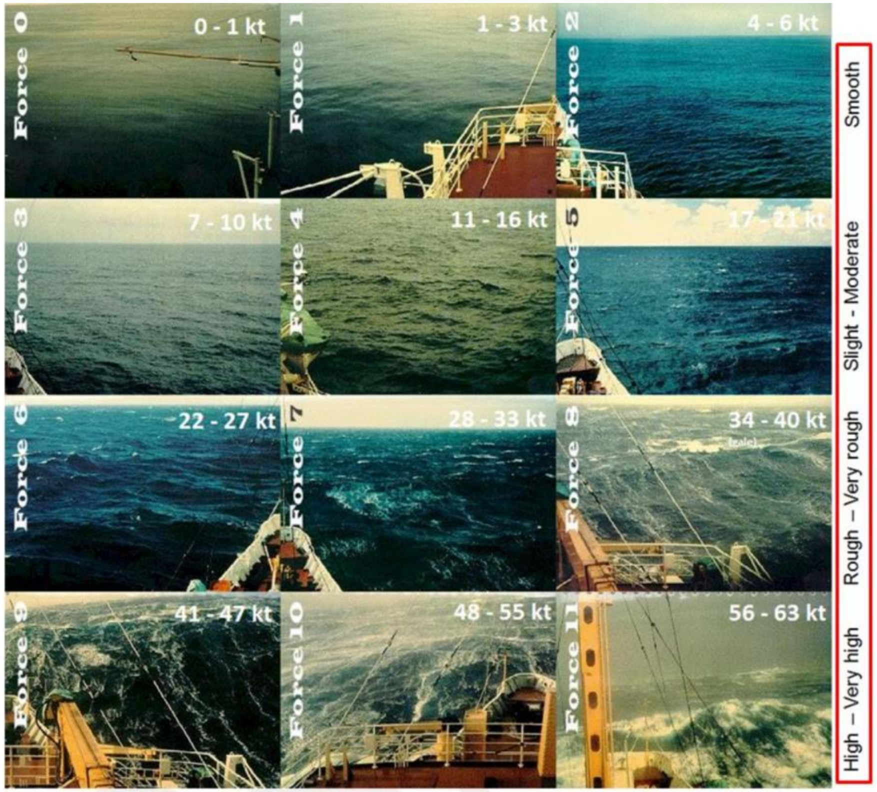

[Douglas sea scale(from World Meteorological Organization) with Beaufort Scale]

Source: Principle of Naval Architecture Vol.III
Douglas sea scale(1921)

Appendix. Related works(~2020)

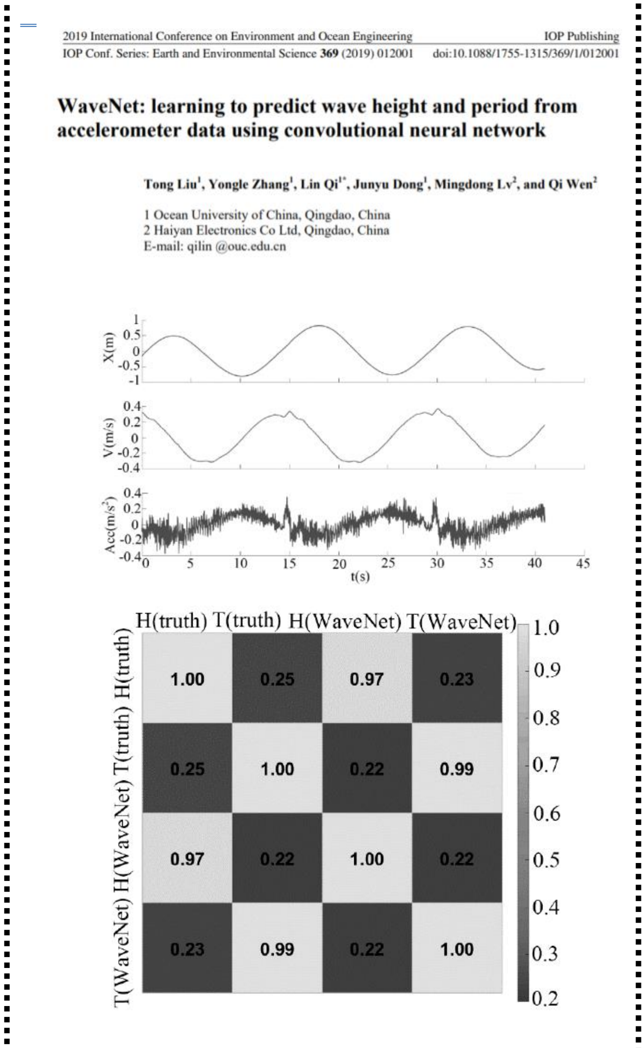

2019 International Conference on Environment and Ocean Engineering — IOP Publishing

IOP Conf. Series: Earth and Environmental Science **369** (2019) 012001 — doi:10.1088/1755-1315/369/1/012001

WaveNet: learning to predict wave height and period from accelerometer data using convolutional neural network

Tong Liu[1], Yongle Zhang[1], Lin Qi[1*], Junyu Dong[1], Mingdong Lv[2], and Qi Wen[2]

1 Ocean University of China, Qingdao, China
2 Haiyan Electronics Co Ltd, Qingdao, China
E-mail: qilin @ouc.edu.cn

	H(truth)	T(truth)	H(WaveNet)	T(WaveNet)
H(truth)	1.00	0.25	0.97	0.23
T(truth)	0.25	1.00	0.22	0.99
H(WaveNet)	0.97	0.22	1.00	0.22
T(WaveNet)	0.23	0.99	0.22	1.00

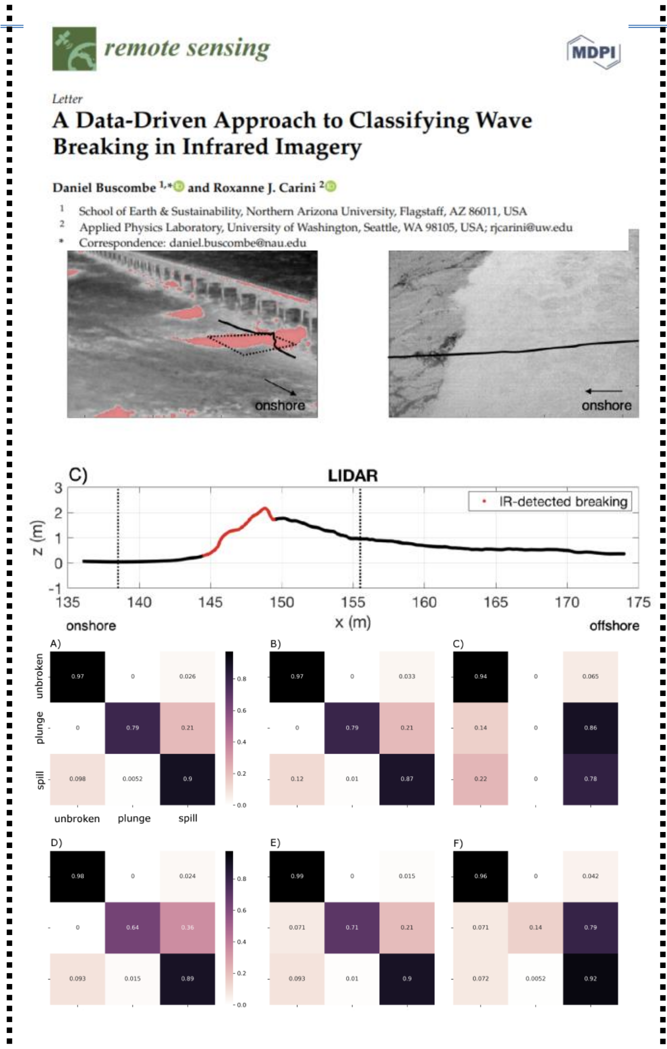

remote sensing — MDPI

Letter

A Data-Driven Approach to Classifying Wave Breaking in Infrared Imagery

Daniel Buscombe [1,*] and Roxanne J. Carini [2]

[1] School of Earth & Sustainability, Northern Arizona University, Flagstaff, AZ 86011, USA
[2] Applied Physics Laboratory, University of Washington, Seattle, WA 98105, USA; rjcarini@uw.edu
* Correspondence: daniel.buscombe@nau.edu

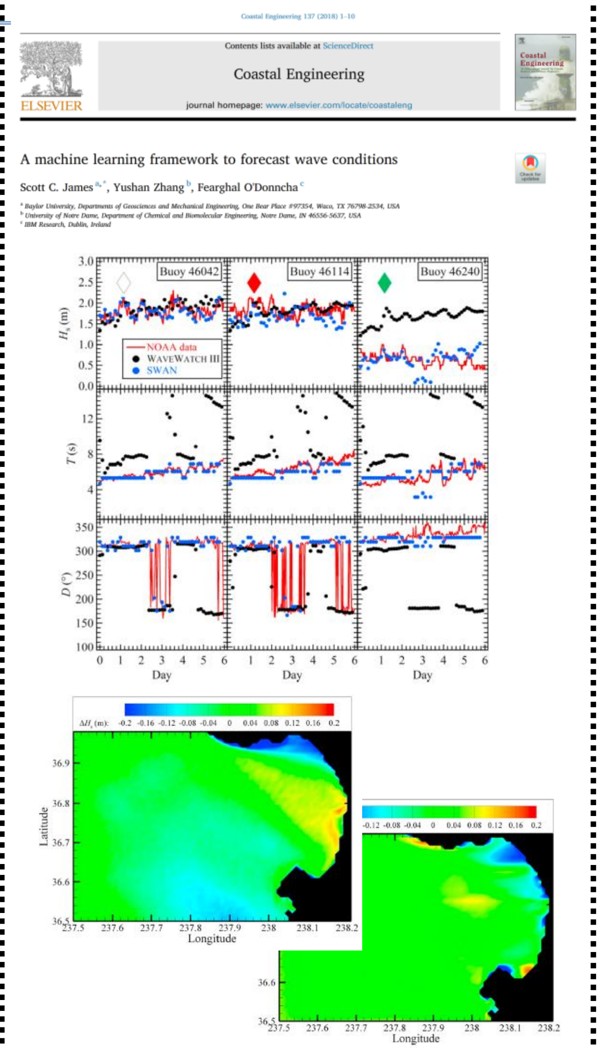

Coastal Engineering 137 (2018) 1–10

Contents lists available at ScienceDirect

Coastal Engineering

journal homepage: www.elsevier.com/locate/coastaleng

ELSEVIER

A machine learning framework to forecast wave conditions

Scott C. James [a,*], Yushan Zhang [b], Fearghal O'Donncha [c]

[a] Baylor University, Departments of Geosciences and Mechanical Engineering, One Bear Place #97354, Waco, TX 76798-2534, USA
[b] University of Notre Dame, Department of Chemical and Biomolecular Engineering, Notre Dame, IN 46556-5637, USA
[c] IBM Research, Dublin, Ireland

- Tong Liu, Yougle Zhang, Lin Qi, Junyu Dong, Mingdong Lv, and Qi Wen. 2019, WaveNet: learning to predict wave height and period from accelerometer data using convolutional neutral network, International Conference on Environment and Ocean Engineering, IOP Conf. Series: Earth and Environmental Science 369, 1-8.
- Daniel Buscombe and Roxanne J. Carini. 2019, A Data-Driven Approach to Classifying Wave Breaking in Infrared Imagery, Remote sensing, 11, 859.
- Scott C. James, Yushan Zhang and Fearghal O’Donncha. 2018, A machine learning framework to forecast wave conditions, Coastal Engineering, 137, 1-10.

Appendix. Related works(2021)

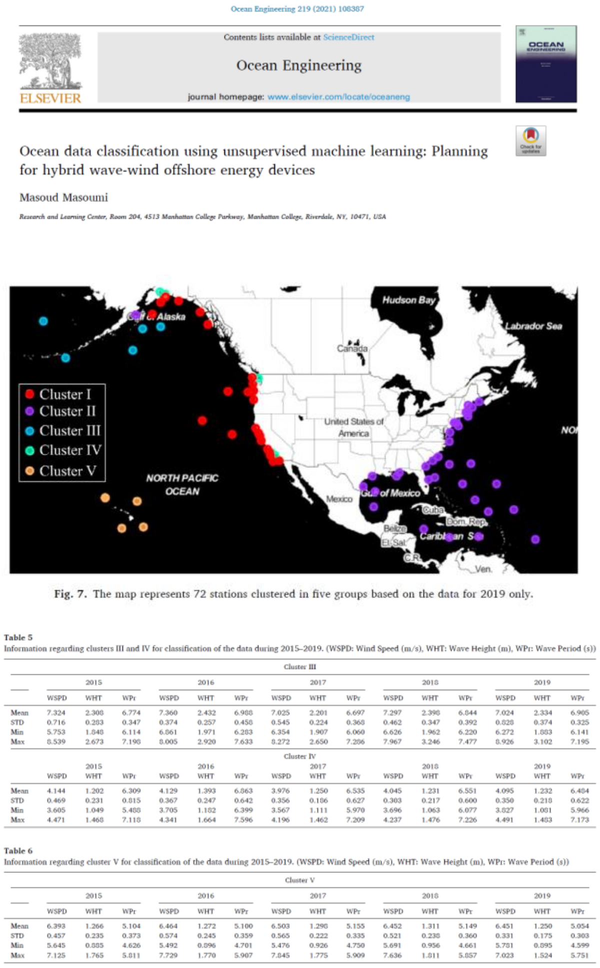

Ocean Engineering 219 (2021) 108387

Contents lists available at ScienceDirect

Ocean Engineering

journal homepage: www.elsevier.com/locate/oceaneng

Ocean data classification using unsupervised machine learning: Planning for hybrid wave-wind offshore energy devices

Masoud Masoumi

Research and Learning Center, Room 204, 4513 Manhattan College Parkway, Manhattan College, Riverdale, NY, 10471, USA

Fig. 7. The map represents 72 stations clustered in five groups based on the data for 2019 only.

Table 5
Information regarding clusters III and IV for classification of the data during 2015–2019. (WSPD: Wind Speed (m/s), WHT: Wave Height (m), WPr: Wave Period (s))

	Cluster III														
	2015			2016			2017			2018			2019		
	WSPD	WHT	WPr	WSPD	WHT	WPr	WSPD	WHT	WPr	WSPD	WHT	WPr	WSPD	WHT	WPr
Mean	7.324	2.308	6.774	7.360	2.432	6.988	7.025	2.201	6.697	7.297	2.398	6.844	7.024	2.334	6.905
STD	0.716	0.283	0.347	0.374	0.257	0.458	0.545	0.224	0.368	0.462	0.347	0.392	0.828	0.374	0.325
Min	5.753	1.848	6.114	6.861	1.971	6.283	6.354	1.907	6.060	6.626	1.962	6.220	6.272	1.883	6.141
Max	8.539	2.673	7.198	8.005	2.920	7.633	8.272	2.650	7.206	7.967	3.246	7.477	8.926	3.102	7.195
	Cluster IV														
	2015			2016			2017			2018			2019		
	WSPD	WHT	WPr	WSPD	WHT	WPr	WSPD	WHT	WPr	WSPD	WHT	WPr	WSPD	WHT	WPr
Mean	4.144	1.202	6.309	4.129	1.393	6.863	3.976	1.250	6.535	4.045	1.231	6.551	4.095	1.232	6.484
STD	0.469	0.231	0.815	0.367	0.247	0.642	0.356	0.186	0.627	0.303	0.217	0.600	0.350	0.218	0.622
Min	3.605	1.049	5.488	3.705	1.182	6.399	3.567	1.111	5.970	3.696	1.063	6.077	3.827	1.081	5.966
Max	4.471	1.468	7.118	4.341	1.664	7.596	4.196	1.462	7.209	4.237	1.476	7.226	4.491	1.483	7.173

Table 6
Information regarding cluster V for classification of the data during 2015–2019. (WSPD: Wind Speed (m/s), WHT: Wave Height (m), WPr: Wave Period (s))

	Cluster V														
	2015			2016			2017			2018			2019		
	WSPD	WHT	WPr	WSPD	WHT	WPr	WSPD	WHT	WPr	WSPD	WHT	WPr	WSPD	WHT	WPr
Mean	6.393	1.266	5.104	6.464	1.272	5.100	6.503	1.298	5.155	6.452	1.311	5.149	6.451	1.250	5.054
STD	0.457	0.235	0.373	0.574	0.245	0.359	0.565	0.222	0.335	0.521	0.238	0.360	0.331	0.175	0.303
Min	5.645	0.885	4.626	5.492	0.896	4.701	5.476	0.926	4.750	5.691	0.956	4.661	5.781	0.895	4.599
Max	7.125	1.765	5.811	7.729	1.770	5.907	7.845	1.775	5.909	7.636	1.811	5.857	7.023	1.524	5.751

- **Data by National Data Buoy Center(NDBC), USA**
- **K-mean clustering**

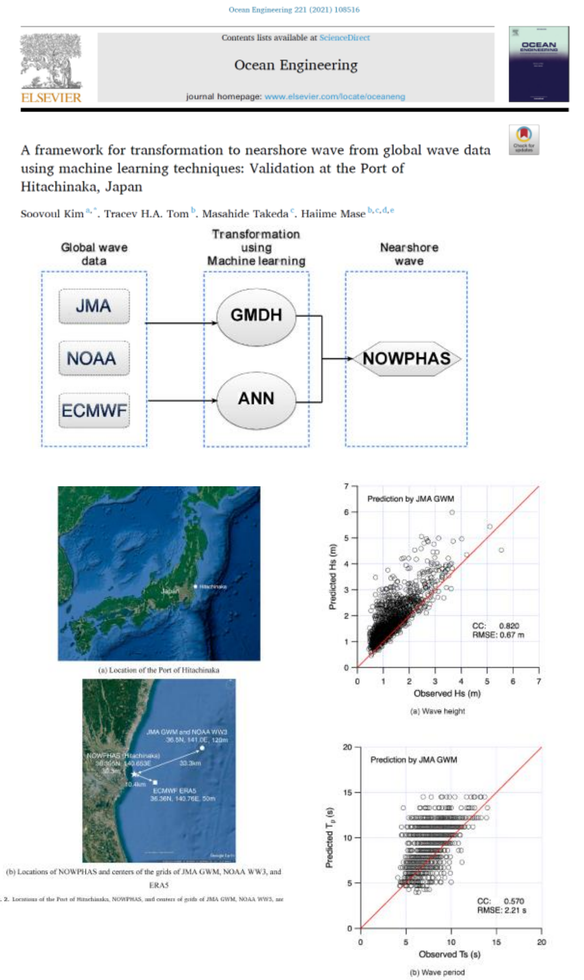

Ocean Engineering 221 (2021) 108516

Contents lists available at ScienceDirect

Ocean Engineering

journal homepage: www.elsevier.com/locate/oceaneng

A framework for transformation to nearshore wave from global wave data using machine learning techniques: Validation at the Port of Hitachinaka, Japan

Soovoul Kim[a,*], Tracev H.A. Tom[b], Masahide Takeda[c], Haiime Mase[b,c,d,e]

(a) Location of the Port of Hitachinaka

(b) Locations of NOWPHAS and centers of the grids of JMA GWM, NOAA WW3, and ERA5

Fig. 2. Locations of the Port of Hitachinaka, NOWPHAS, and centers of grids of JMA GWM, NOAA WW3, and

(a) Wave height

(b) Wave period

Fig. 5. Comparisons between global wave data of JMA GWM and observed nearshore wave data (NOWPHAS).

- **Hindcasting** of wave height, period at the nearshore
- **ANN** and **Group method of data handling**(GMDH)

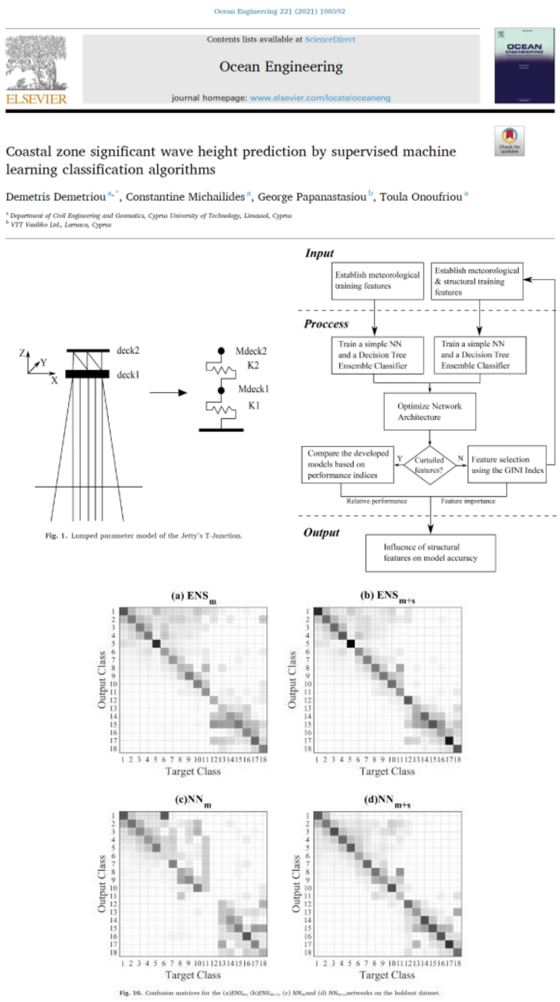

Ocean Engineering 221 (2021) 108592

Contents lists available at ScienceDirect

Ocean Engineering

journal homepage: www.elsevier.com/locate/oceaneng

Coastal zone significant wave height prediction by supervised machine learning classification algorithms

Demetris Demetriou[a,*], Constantine Michailides[a], George Papanastasiou[b], Toula Onoufriou[a]

[a] Department of Civil Engineering and Geomatics, Cyprus University of Technology, Limassol, Cyprus
[b] VTT Vasiliko Ltd., Larnaca, Cyprus

Fig. 1. Lumped parameter model of the Jetty's T-Junction.

Fig. 10. Confusion matrices for the (a)ENS_m, (b)ENS_{m+s}, (c) NN_m and (d) NN_{m+s} networks on the holdout dataset.

- **Structural data** for significant wave height **prediction**
- **ANN** and **Decision tree model**

Appendix. Related works(2021)

Article

Skilful precipitation nowcasting using deep generative models of radar

https://doi.org/10.1038/s41586-021-03854-z

Received: 17 February 2021

Accepted: 27 July 2021

Published online: 29 September 2021

Suman Ravuri[1,5], Karel Lenc[1,5], Matthew Willson[1,5], Dmitry Kangin[2,3], Remi Lam[1], Piotr Mirowski[1], Megan Fitzsimons[2], Maria Athanassiadou[2], Sheleem Kashem[1], Sam Madge[2], Rachel Prudden[2,3], Amol Mandhane[1], Aidan Clark[1], Andrew Brock[1], Karen Simonyan[1], Raia Hadsell[1], Niall Robinson[2,3], Ellen Clancy[1], Alberto Arribas[2,4] & Shakir Mohamed[1]✉

- **Deep generative model** for the probabilistic nowcasting of precipitation form radar
- Improved forecast quality
- **1,536km X 1,280km**, **5-90min** forecasting

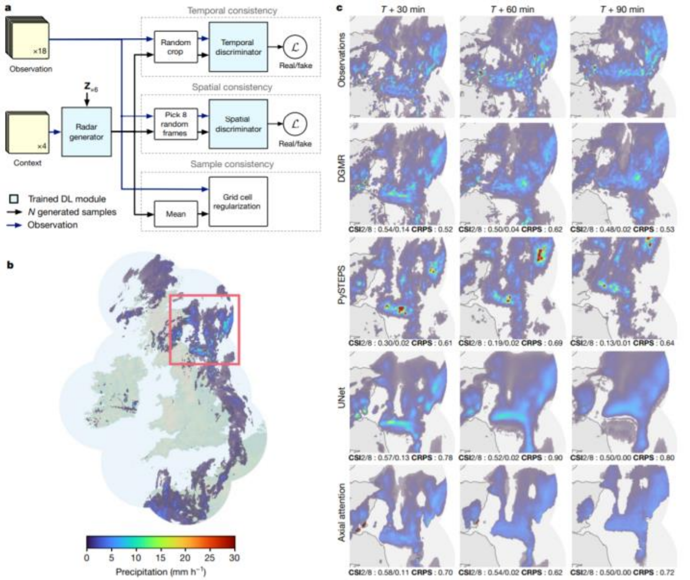

Fig. 1 | Model overview and case study of performance on a challenging precipitation event starting on = 24 June 2019 at 16:15 UK, showing convective cells over eastern Scotland. DGMR is better able to predict the spatial coverage and convection compared to other methods over a longer time period, while not over-estimating the intensities, and is significantly preferred by meteorologists (93% first choice, $n = 56$, $P < 10^{-4}$). **a**, Schematic of the model architecture showing the generator with spatial latent vectors **Z**. **b**, Geographic context for the predictions. **c**, A single prediction at $T + 30$, $T + 60$ and $T + 90$ min lead time for different models. Critical success index (CSI) at thresholds 2 mm h^{-1} and 8 mm h^{-1} and continuous ranked probability score (CRPS) for an ensemble of four samples shown in the bottom left corner. For axial attention we show the mode prediction. Images are 256 km × 256 km. Maps produced with Cartopy and SRTM elevation data[46].

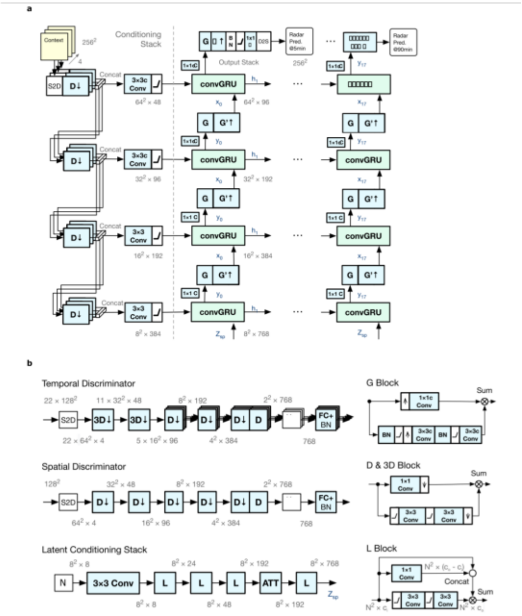

Extended Data Fig. 1 | Detailed architecture of DGMR. a, Generator architecture. S2D is space-to-depth operation; D2S is depth to space. **b**, Temporal discriminator architecture (top left), spatial discriminator (middle left), and latent conditioning stack (bottom left) of the generator. On the right are architectures for the G block (top), D and 3D block (middle), and L block (right). For all panels, (↑) or (↓) indicates spatial up-sampling or down-sampling, respectively.

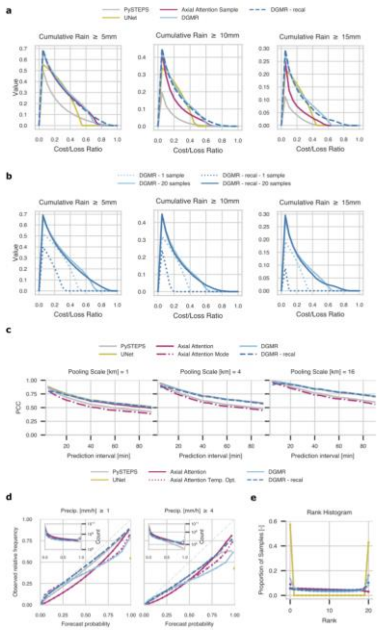

Extended Data Fig. 4 | Further verification scores for the UK in 2019. a, Comparison of relative economic value across 20 samples of different models for different rain accumulations. UNet generates a single deterministic prediction. **b**, Effect of larger ensemble in increasing economic value. **c**, Pearson correlation coefficient of various models at grid-resolution (left), rain rates averaged over a 4 km aggregation (middle) and averaged over a 16 km aggregation (right). **d**, Reliability diagrams and sharpness plots for two precipitation thresholds for $T + 60$ min predictions. **e**, Rank histogram at $T + 60$ min.

Source: Suman Ravuri et al.(2021). Skilful precipitation nowcasting using deep generative models of radar. NATURE. 597. 672-677.

Appendix. Layers of CNN

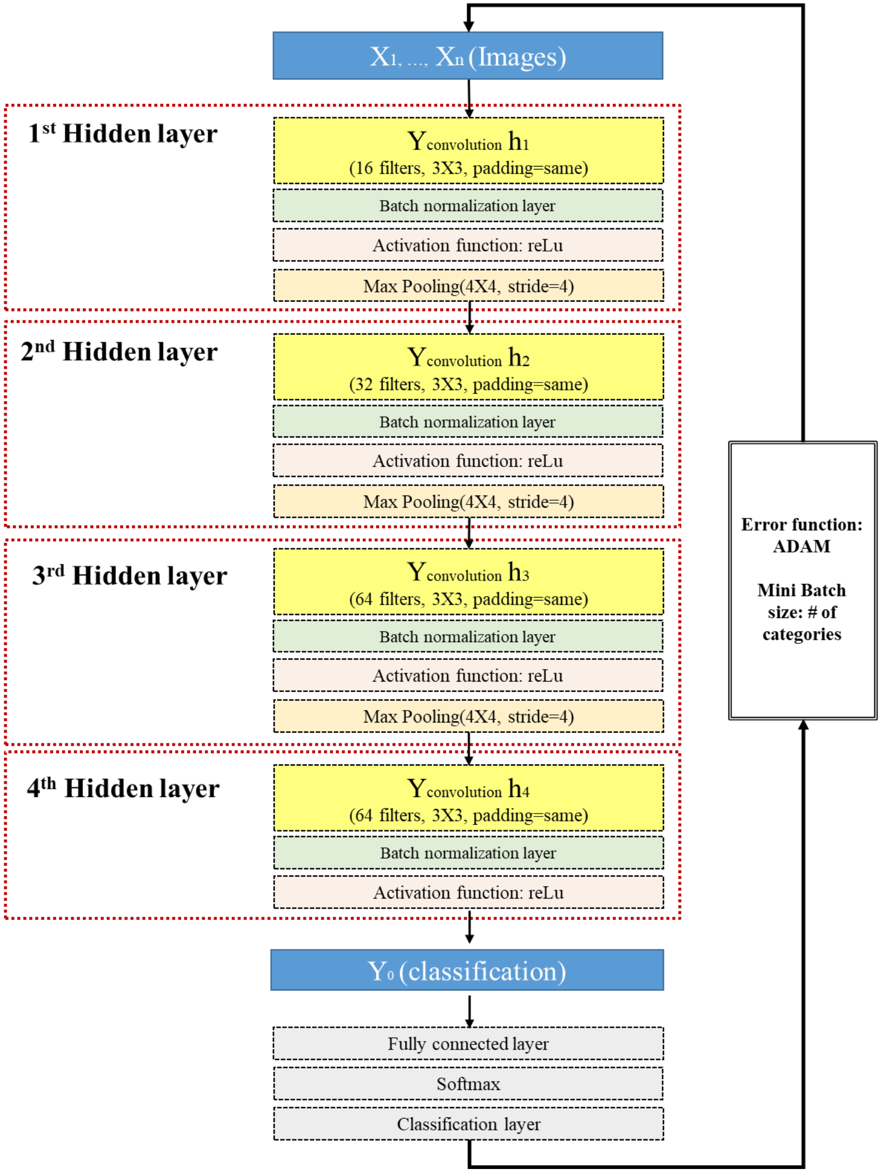

$X_1, \ldots, X_n$ (Images)

1st Hidden layer

$Y_{\text{convolution}}$ h_1
(16 filters, 3X3, padding=same)

Batch normalization layer

Activation function: reLu

Max Pooling(4X4, stride=4)

2nd Hidden layer

$Y_{\text{convolution}}$ h_2
(32 filters, 3X3, padding=same)

Batch normalization layer

Activation function: reLu

Max Pooling(4X4, stride=4)

3rd Hidden layer

$Y_{\text{convolution}}$ h_3
(64 filters, 3X3, padding=same)

Batch normalization layer

Activation function: reLu

Max Pooling(4X4, stride=4)

4th Hidden layer

$Y_{\text{convolution}}$ h_4
(64 filters, 3X3, padding=same)

Batch normalization layer

Activation function: reLu

Y_0 (classification)

Fully connected layer

Softmax

Classification layer

Error function: ADAM

Mini Batch size: # of categories

Convolution layer

The layer convolves the input by moving the filters along the input vertically and horizontally and computing the dot product of the weights and the input, and then adding a bias term

Batch normalization layer

It normalizes each input channel across a mini-batch for speeding up training of convolutional neural networks and reducing the sensitivity to network initialization.

Activation function

$$f(x) = \begin{cases} x, x \geq 0 \\ 0, x < 0 \end{cases}$$

It performs a threshold operation to each element of the input, where any value less than zero is set to zero.

Max Pooling

It performs down-sampling by dividing the input into rectangular pooling regions, and computing the maximum of each region.

Fully connected layer

It multiplies the input by a weight matrix and then adds a bias vector.

Softmax

$$S(y_i) = \frac{e^{y_i}}{\sum_{j=1}^{i} e^{y_j}}$$

It applies a softmax function to the input. Softmax function converts a vector of numbers into a vector of possibilities.

Classification layer

It computes the cross entropy loss for multi-class classification problems with mutually exclusive classes. The layer infers the number of classes from the output size of the previous layer.

Error function: ADAM

$$m_i = \beta_1 m_{i-1} + (1-\beta_1)\nabla E(\theta_i)$$

$$v_i = \beta_2 v_{i-1} + (1-\beta_2)[\nabla E(\theta_i)]^2$$

Adam (adaptive moment estimation): An element-wise moving average of both the parameter gradients and their squared values.

$$\theta_{i+1} = \theta_i - \frac{\alpha m_i}{\sqrt{v_i} + \varepsilon}$$

Appendix. Initial CNN numerical setup & computing environment

Base model	AlexNet
Learning method	CNN(Convolution Neutral Network)
Number of convolution layer	4
Solver	**ADAM(Adaptive Moment Estimation)**
Activation function	**ReLU(Rectified Linear Unit)**
Number of filters per each convolution layer	16 / 32 / 64 / 64 4X4 with same padding
Max pooling	1st, 2nd, 3rd: 4X4 with 4 stride
Gradient Decay Factor	**0.9**
Squared Gradient Decay Factor	**0.999**
Gradient Threshold Method	L_2 norm
Epoch	**8**
Mini-batch size	**3 times of number of categories**

Characteristics of Graphics Processing Unit(GPU)	
Name	GeForce RTX 2080 SUPER
Max Grid Size	[2.1475e09 65535 65535]
Total Memory [bytes]	8.5899e09
Available Memory [bytes]	6.8783e09
Multiprocessor Count	48
Clock Rate [kHz]	1.8300e06
General Information of Personal Computer(PC)	
Operating System(OS)	Windows 10 Enterprise
Processor	AMD Ryzen 9 3900X 12-Core Processor / 3.80GHz
RAM [GB]	63.9
System Type	64 bit OS / x64 based Processor

ADAM

$$m_i = \beta_1 m_{i-1} + (1-\beta_1)\nabla E(\theta_i)$$
$$v_i = \beta_2 v_{i-1} + (1-\beta_2)[\nabla E(\theta_i)]^2$$

$$\theta_{i+1} = \theta_i - \frac{\alpha m_i}{\sqrt{v_i} + \varepsilon}$$

ReLU

$$f(x) = \begin{cases} x, x \geq 0 \\ 0, x < 0 \end{cases}$$

Appendix. GoogLeNet

- **GoogLeNet(2014)**
  - 2014 ILSVRC winning algorithm
  - 22-layer deep model
  - Features
    - 1 X 1 convolution for reducing feature map
    - Inception module for feature extraction
    - Global average pooling for flattening with lower computing(compared to FC)
    - Auxiliary classifier for avoiding vanishing gradient

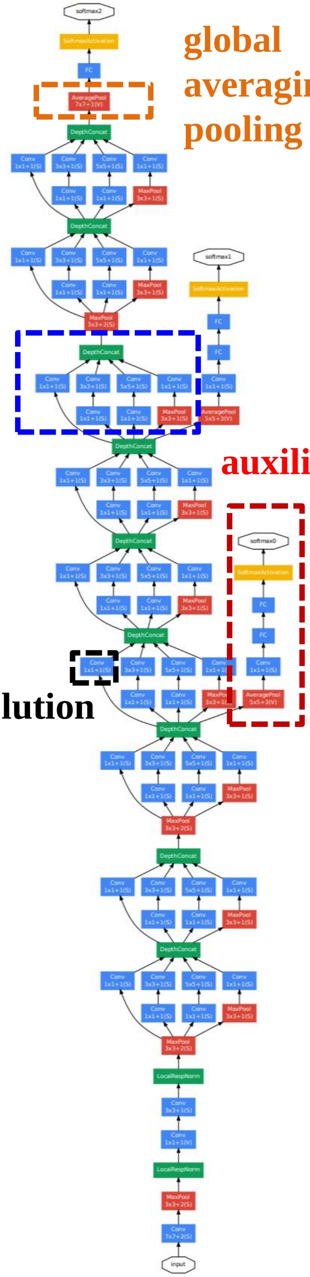

global averaging pooling

inception module

auxiliary classifier

1X1 convolution

[GoogLeNet network(2015)]

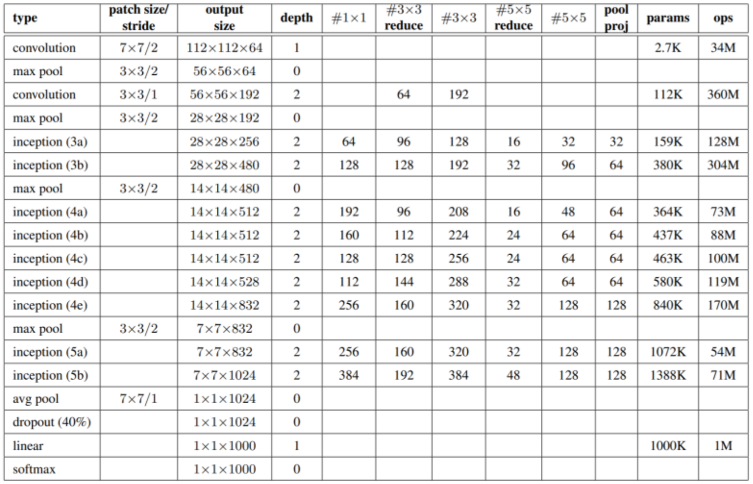

type	patch size/ stride	output size	depth	#1×1	#3×3 reduce	#3×3	#5×5 reduce	#5×5	pool proj	params	ops
convolution	7×7/2	112×112×64	1							2.7K	34M
max pool	3×3/2	56×56×64	0								
convolution	3×3/1	56×56×192	2		64	192				112K	360M
max pool	3×3/2	28×28×192	0								
inception (3a)		28×28×256	2	64	96	128	16	32	32	159K	128M
inception (3b)		28×28×480	2	128	128	192	32	96	64	380K	304M
max pool	3×3/2	14×14×480	0								
inception (4a)		14×14×512	2	192	96	208	16	48	64	364K	73M
inception (4b)		14×14×512	2	160	112	224	24	64	64	437K	88M
inception (4c)		14×14×512	2	128	128	256	24	64	64	463K	100M
inception (4d)		14×14×528	2	112	144	288	32	64	64	580K	119M
inception (4e)		14×14×832	2	256	160	320	32	128	128	840K	170M
max pool	3×3/2	7×7×832	0								
inception (5a)		7×7×832	2	256	160	320	32	128	128	1072K	54M
inception (5b)		7×7×1024	2	384	192	384	48	128	128	1388K	71M
avg pool	7×7/1	1×1×1024	0								
dropout (40%)		1×1×1024	0								
linear		1×1×1000	1							1000K	1M
softmax		1×1×1000	0								

[GoogLeNet incarnation of the inception architecture(2015)]

Appendix. Long Short-Term Memory(LSTM)

- **Long Short-Term Memory(LSTM)**
  - RNN based deep learning
  - 3 additional inner gates, 1 cell state in each hidden layer
    - Forget gate
    - Input gate
    - Output gate
    - (cell) state

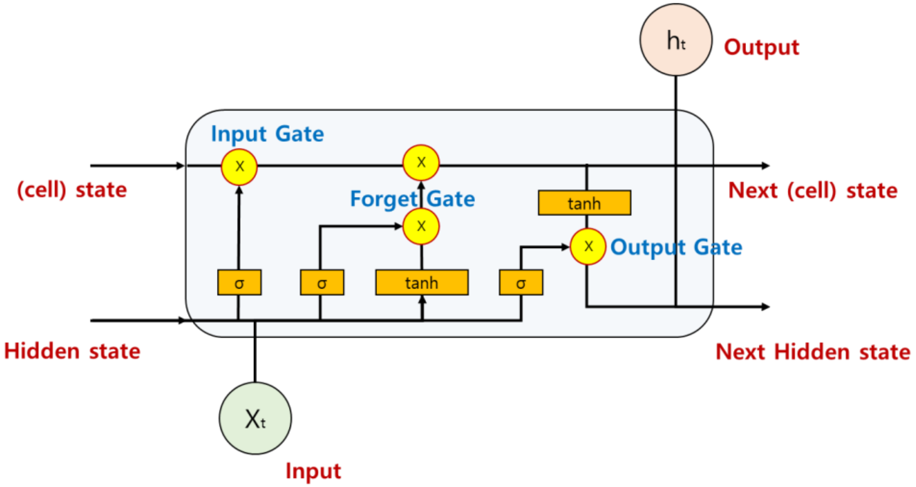

[Hochreiter & Schmidhuber(1997)]

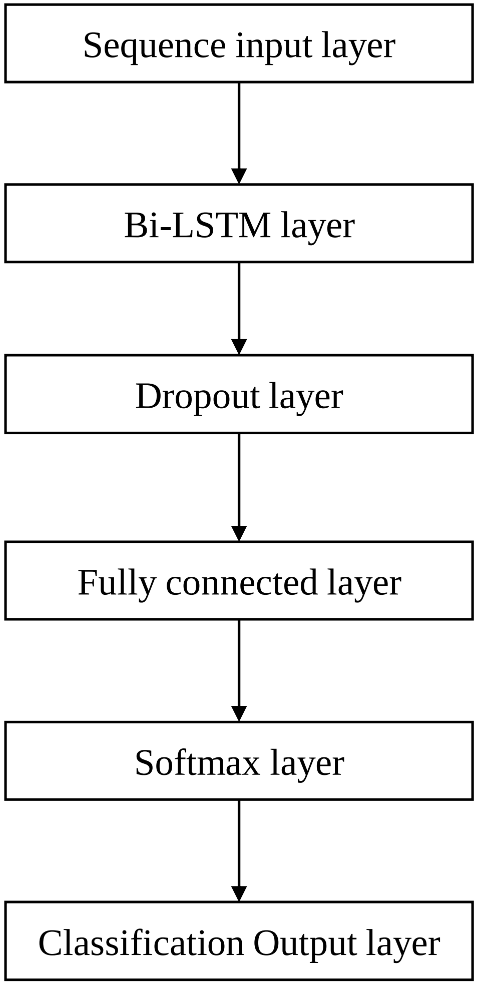

Sequence input layer — Sequence length: 1024

Bi-LSTM layer

<u>**Hyper-parameter**</u>
Input Size: 'auto'
Num Hidden Units: 2000
Output Mode: 'last'
State Activation Function: 'tanh'
Gate Activation Function: 'sigmoid'

Dropout layer — Dropout probability: 0.5

Fully connected layer

Input size: auto
Output size: Number of categories

Softmax layer

Classification Output layer — Loss function: Cross entropy loss

[LSTM network]

Appendix. Training options of LSTM

Item	Option
Learning method	LSTM(Long Short-Term Memory)
Optimizer	ADAM(Adaptive Moment Estimation)
Gradient Decay Factor	0.9000
Squared Gradient Decay Factor	0.9990
Epsilon	1.0000e-08
Initial Learn Rate	1.0000e-04
Learn Rate Schedule	None
Learn Rate Drop Factor	0.1000
Learn Rate Drop Period	10
L_2 Regularization	1.0000e-04
Gradient Threshold Method	L_2 norm
Gradient Threshold	2
Max Epochs	200
Mini Batch Size	4
Verbose	1
Verbose Frequency	20
Validation Data	{{37X1 cell} [37X1 categorical]}
Validation Frequency	81
Validation Patience	Inf
Shuffle	‘every-epoch’
Execution Environment	‘auto’
Plots	‘training-progress’
Sequence Length	‘longest’
Sequence Padding Value	0
Sequence Padding Direction	‘right’
Dispatch in Background	0

Appendix. Numerical wave by Airy waves

Source: DNVGL-RP-C205 "Environmental Conditions and Environmental Loads

- **Wave field generation**

$$S(\omega) = \frac{5}{16}\left(1 - 0.287\ln(\gamma)\right){H_S}^2{\omega_P}^{-4}\omega^{-5}e^{\left[-1.25\left(\frac{\omega}{\omega_P}\right)^{-4}\right]}\gamma^{e^{\left[\frac{-(\omega-\omega_P)^2}{2\sigma^2{\omega_P}^2}\right]}}$$

$$A(\omega_i) = \sqrt{2S(\omega_i)\Delta\omega}$$

$$\theta(\omega_i) = Randomly\ distributed$$

$$\eta(t) = \sum_{i=1}^{N} A(\omega_i)\cos(\omega_i t + \theta(\omega_i))$$

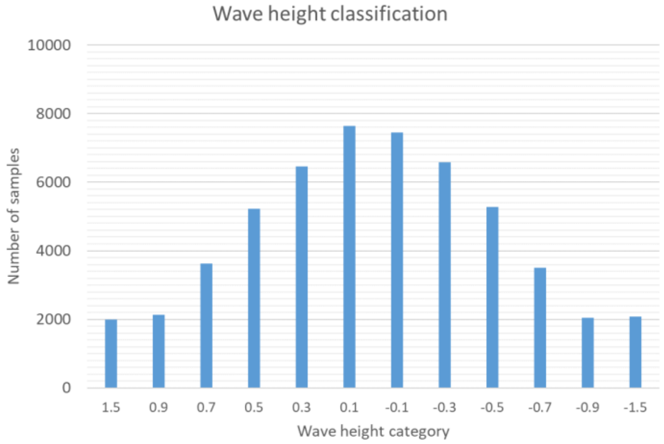

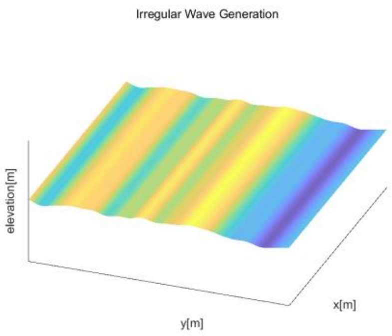

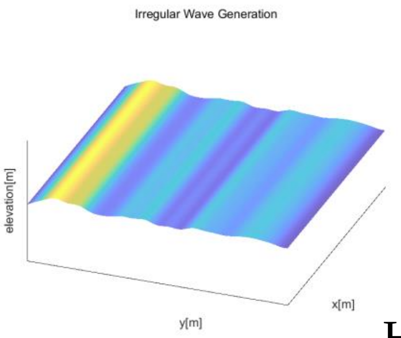

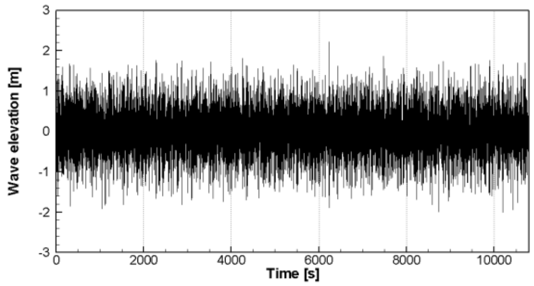

Hs=2.4m, Tp=6.6s, Gamma=2.5

Appendix. Numerical wave by Airy waves

- **Short-crested waves prediction**

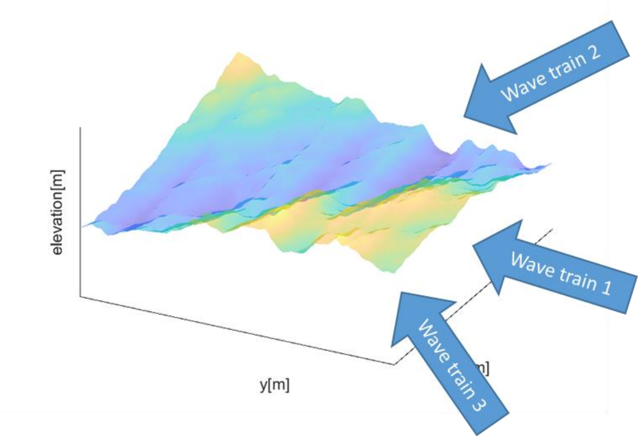

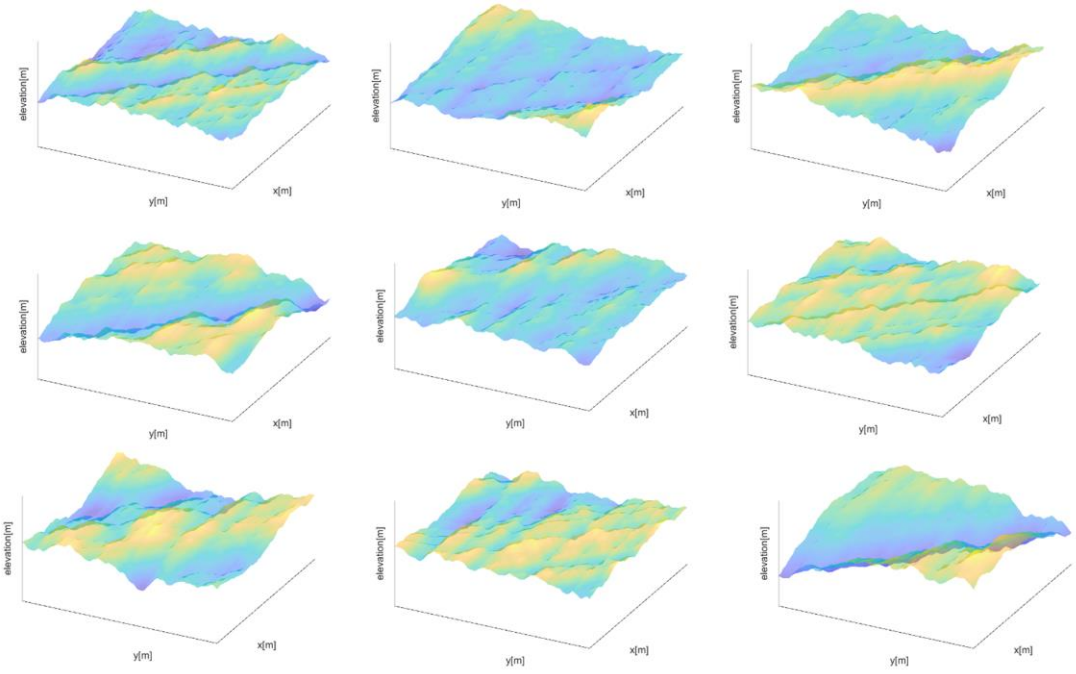

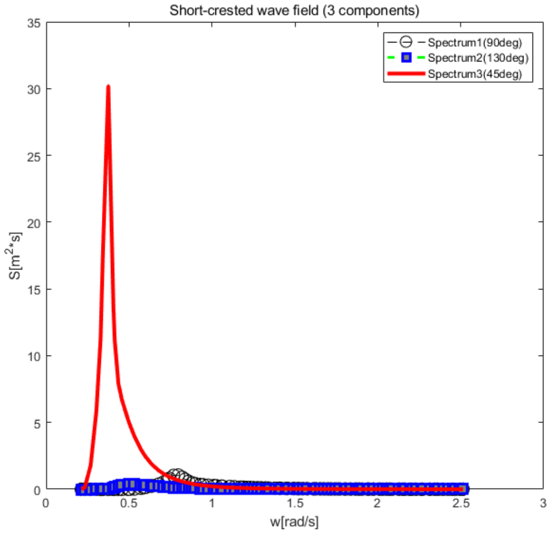

	Hs [m]	Tp [s]	Gamma	Dir. [°]
Wave train 1	2.4	8.0	2.5	90
Wave train 2	1.8	12.0	2.5	130
Wave train 3	7.7	17.0	3.3	45

$$S(\omega,\theta)=\sum_{i=1}^{n} S_i(\omega)D_i(\omega,\theta)$$

$$\int_{\theta} D_i(\omega,\theta)d\theta = 1$$

Appendix. Pattern tracking algorithm

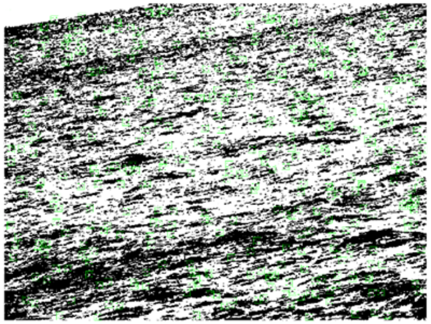

BRISK (Stefan L. et al, 2011)

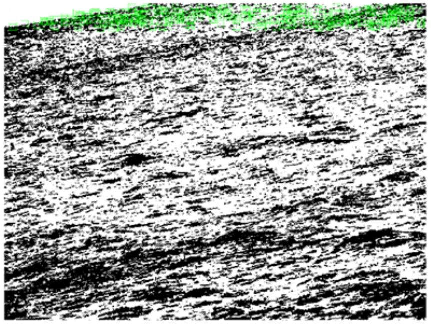

FAST (Edward R. and Tom D., 2005)

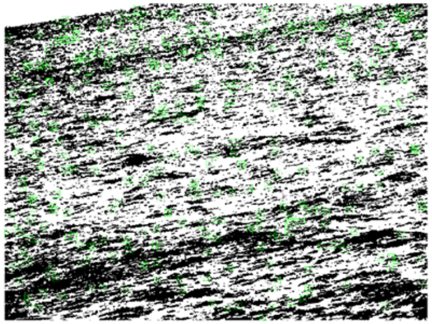

Harris (Harris C. and M. Stephens, 1988)

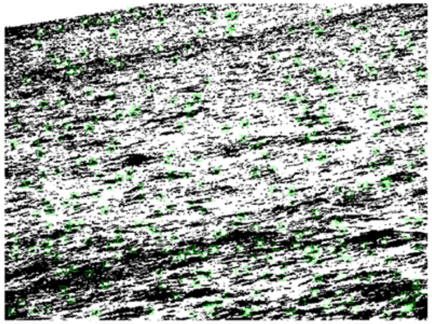

KAZE (Alcantarilla PF. et al, 2012)

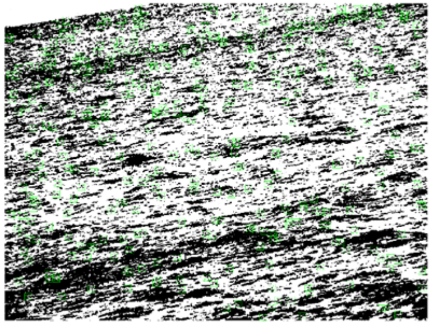

Minimum Eigenvalue (Shi J. and C. Tomasi, 1994)

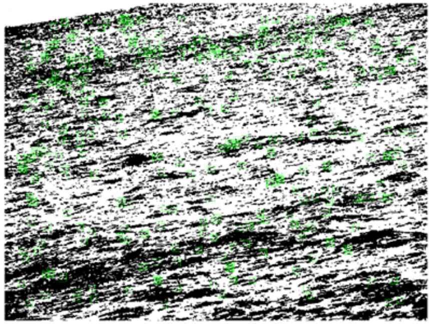

ORB (Rublee E. et al, 2011)

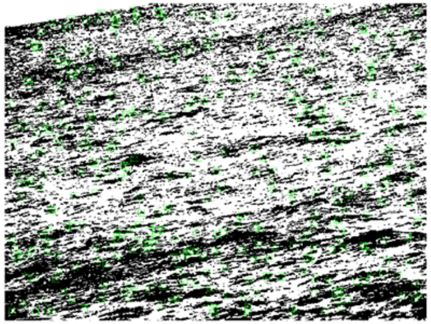

SURF (Bay H. et al, 2008)